Channel Estimation for Wireless OFDM Communications

Jia-Chin Lin
National Central University
Taiwan

1. Introduction

1.1 Preliminary

Orthogonal frequency-division multiplexing (OFDM) communication techniques have recently received significant research attention because of their ability to maintain effective transmission and highly efficient bandwidth utilization in the presence of various channel impairments, such as severely frequency-selective channel fades caused by long multipath delay spreads and impulsive noise (Bingham, 1990; Zou & Wu, 1995). In an OFDM system, a high-rate serial information-bearing symbol stream is split into many low-rate parallel streams; each of these streams individually modulates a mutually orthogonal sub-carrier. The spectrum of an individual sub-channel overlaps with those expanded from the adjacent sub-channels. However, the OFDM sub-carriers are orthogonal as long as they are synthesized such that the frequency separation between any two adjacent sub-carriers is exactly equal to the reciprocal of an OFDM block duration. A discrete Fourier transform (DFT) operation can perfectly produce this sub-carrier arrangement and its relevant modulations (Darlington, 1970; Weinstein & Ebert, 1971). Because of the advanced technologies incorporated into integrated circuit (IC) chips and digital signal processors (DSPs), OFDM has become a practical way to implement very effective modulation techniques for various applications. As a result, OFDM technologies have recently been chosen as candidates for 4th-generation (4G) mobile communications in a variety of standards, such as IEEE 802.16 (Marks, 2008) and IEEE 802.20 (Klerer, 2005) in the United States, and international research projects, such as EU-IST-MATRICE (MATRICE, 2005) and EU-IST-4MORE (4MORE, 2005) for 4G mobile communication standardization in Europe.

Regarding the history of OFDM, recall that Chang published a paper on the synthesis of band-limited signals for parallel multi-channel transmission in the 1960s (Chang, 1966). The author investigated a technique for transmitting and receiving (transceiving) parallel information through a linear band-limited channel without inter-channel interference (ICI) or inter-symbol interference (ISI). Saltzberg then conducted relevant performance evaluations and analyses (Saltzberg, 1967).

1.2 IFFT and FFT utilization: A/D realization of OFDM

A significant breakthrough in OFDM applicability was presented by Weinstein and Ebert in 1971 (Weinstein & Ebert, 1971). First, DFT and inverse DFT (IDFT) techniques were applied

to OFDM implementation to perform base-band parallel sub-channel modulations and demodulations (or multiplexing and demultiplexing) (Weinstein & Ebert, 1971). This study provided an effective discrete-time signal processing method to simultaneously modulate (and demodulate) signals transmitted (and received) on various sub-channels without requiring the implementation of a bank of sub-carrier modulators with many analog multipliers and oscillators. Meanwhile, ISI can be significantly reduced by inserting a guard time-interval (GI) in between any two consecutive OFDM symbols and by applying a raised-cosine windowing method to the time-domain (TD) signals (Weinstein & Ebert, 1971). Although the system studied in this work cannot always maintain orthogonality among sub-carriers when operated over a time-dispersive channel, the application of IDFT and DFT to OFDM communication is not only a crucial contribution but also a critical driving force for commercial applicability of recent wireless OFDM communication because the fast algorithms of IDFT and DFT, i.e., inverse fast Fourier transform (IFFT) and fast Fourier transform (FFT), have been commercialized and popularly implemented with ASICs or sub-functions on DSPs.

1.3 Cyclic prefix

Orthogonality among sub-carriers cannot be maintained when an OFDM system operates over a time-dispersive channel. This problem was first addressed by Peled and Ruiz in 1980 (Peled & Ruiz, 1980). Rather than inserting a blank GI between any two consecutive OFDM symbols, which was the method employed in the previous study (Weinstein & Ebert, 1971), a cyclic extension of an OFDM block is inserted into the original GI as a prefix to an information-bearing OFDM block. The adopted cyclic prefix (CP) effectively converts the linear convolution of the transmitted symbol and the channel impulse response (CIR) into the cyclic convolution; thus, orthogonality among sub-carriers can be maintained with channel time-dispersion if the CP is sufficiently longer than the CIR. However, energy efficiency is inevitably sacrificed, as the CPs convey no desired information.

1.4 Applications

OFDM technology is currently employed in the European digital audio broadcasting (DAB) standard (DAB, 1995). In addition, digital TV broadcasting applications based on OFDM technology have been under comprehensive investigation (DVB, 1996; Couasnon et al., 1994; Marti et al., 1993; Moeneclaey & Bladel, 1993; Tourtier et al., 1993). Furthermore, OFDM technology in conjunction with other multiple-access techniques, in particular code-division multiple-access (CDMA) techniques, for mobile communications has also been the focus of a variety of research efforts (Hara & Prasad, 1997; Sourour & Nakagawa, 1996; Kondo & Milstein, 1996; Reiners & Rohling, 1994; Fazel, 1994). For those employed in wireline environments, OFDM communication systems are often called "Discrete Multi-Tone" (DMT) communications, which have also attracted a great deal of research attention as a technology that effectively achieves high-rate transmission on currently existing telephone networks (Bingham, 1990; Young et al., 1996; Chow, 1993; Tu, 1991). One of the major advantages of the OFDM technique is its robustness with multipath reception. OFDM applications often are expected to operate in a severely frequency-selective environment. Therefore, OFDM communication has recently been selected for various broadband mobile communications, e.g., 4G mobile communications. This chapter will focus on such applications.

1.5 System description and signal modelling

The primary idea behind OFDM communication is dividing an occupied frequency band into many parallel sub-channels to deliver information simultaneously. By maintaining sufficiently narrow sub-channel bandwidths, the signal propagating through an individual sub-channel experiences roughly frequency-flat (i.e., frequency-nonselective) channel fades. This arrangement can significantly reduce the complexity of the subsequent equalization sub-system. In particular, current broadband wireless communications are expected to be able to operate in severe multipath fading environments in which long delay spreads inherently exist because the signature/chip duration has become increasingly shorter. To enhance spectral (or bandwidth) efficiency, the spectra of adjacent sub-channels are set to overlap with one another. Meanwhile, the orthogonality among sub-carriers is maintained by setting the sub-carrier spacing (i.e., the frequency separation between two consecutive sub-carriers) to the reciprocal of an OFDM block duration.

By taking advantage of a CP, the orthogonality can be prevented from experiencing ICI even for transmission over a multipath channel (Peled & Ruiz, 1980). Although several variants of OFDM communication systems exist (Bingham, 1990; Weinstein & Ebert, 1971; Floch et al., 1995), CP-OFDM (Peled & Ruiz, 1980) is primarily considered in this section due to its popularity. A CP is obtained from the tail portion of an OFDM block and then prefixed into a transmitted block, as shown in Fig. 1.
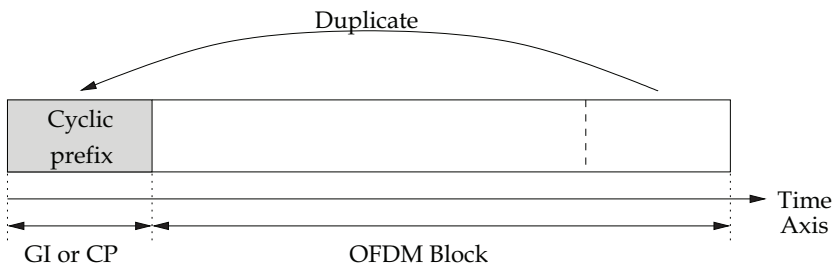

Fig. 1. An OFDM symbol consisting of a CP and an information-bearing OFDM block.

A portion of the transmitted OFDM symbol becomes periodic. The CP insertion converts the linear convolution of the CIR and the transmitted symbol into the circular convolution of the two. Therefore, CPs can avoid both ISI and ICI (Bingham, 1990). In this fundamental section, the following assumptions are made for simplicity: (1) a cyclic prefix is used; (2) the CIR length does not exceed the CP length; (3) the received signal can be perfectly synchronized; (4) noise is complex-valued, additive, white Gaussian noise (AWGN); and (5) channel time-variation is slow, so the channel can be considered to be constant or static within a few OFDM symbols.

1.5.1 Continuous-time model

A continuous-time base-band equivalent representation of an OFDM transceiver is depicted in Fig. 2. The OFDM communication system under study consists of N sub-carriers that occupy a total bandwidth of $B = \frac{1}{T_s}$ Hz. The length of an OFDM symbol is set to T_{sym} seconds; moreover, an OFDM symbol is composed of an OFDM block of length $T = NT_s$ and a CP of length T_g. The transmitting filter on the kth sub-carrier can be written as

$$p_k(t) = \begin{cases} \dfrac{1}{\sqrt{T}} e^{j2\pi \frac{B}{N}k(t-T_g)} & 0 \le t \le T_{sym} \\ 0 & \text{otherwise,} \end{cases} \tag{1}$$

where $T_{sym} = T + T_g$. Note that $p_k(t) = p_k(t+ T)$ when t is within the guard interval $[0,T_g]$. It can be seen from Equation 1 that $p_k(t)$ is a rectangular pulse modulated by a sub-carrier with frequency $k \cdot \frac{B}{N}$. The transmitted signal $s_i(t)$ for the ith OFDM symbol can thus be obtained by summing over all modulated signals, i.e.,

$$s_i(t) = \sum_{k=0}^{N-1} X_{k,i} p_k\left(t - iT_{sym}\right), \tag{2}$$

where $X_{0,i}, X_{1,i}, \cdots, X_{N-1,i}$ are complex-valued information-bearing symbols, whose values are often mapped according to quaternary phase-shift keying (QPSK) or quadrature amplitude modulation (QAM). Therefore, the transmitted signal $s(t)$ can be considered to be a sequence of OFDM symbols, i.e.,

$$\begin{aligned} s(t) &= \sum_{i=-\infty}^{\infty} s_i(t) \\ &= \sum_{i=-\infty}^{\infty} \sum_{k=0}^{N-1} X_{k,i} p_k\left(t - iT_{sym}\right). \end{aligned} \tag{3}$$
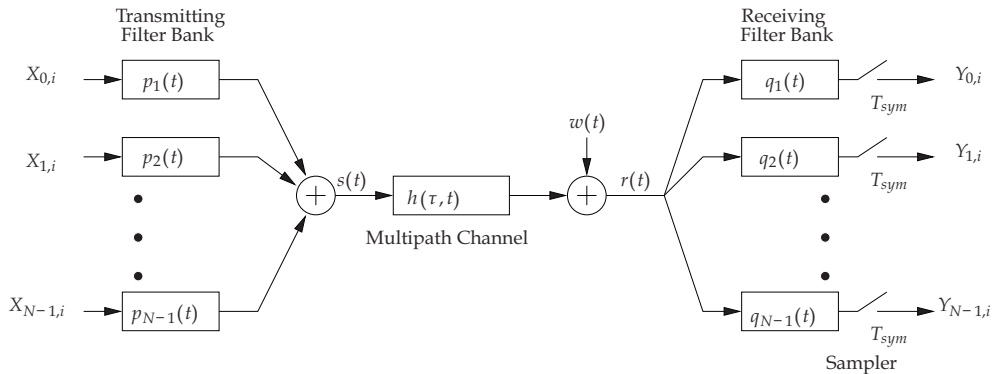

Fig. 2. Continuous-time base-band equivalent representation of an OFDM transceiver.

If the length of the CIR $h(\tau, t)$ does not exceed the CP length T_g, the received signal $r(t)$ can be written as

$$\begin{aligned} r(t) &= \left(h * s\right)(t) + w(t) \\ &= \int_0^{T_g} h(\tau,t)s(t-\tau)d\tau + w(t), \end{aligned} \tag{4}$$

where the operator "$*$" represents the linear convolution and $w(t)$ is an AWGN.

At the receiving end, a bank of filters is employed to match the last part $[T_g, T_{sym}]$ of the transmitted waveforms $p_k(t)$ on a subchannel-by-subchannel basis. By taking advantage of

matched filter (MF) theory, the receiving filter on the kth sub-channel can be designed to have the following impulse response:

$$q_k(t) = \begin{cases} p_k^*\left(T_{sym} - t\right), & 0 \le t < T = T_{sym} - T_g \\ 0, & \text{otherwise.} \end{cases} \tag{5}$$

Because the CP can effectively separate symbol dispersion from preceding or succeeding symbols, the sampled outputs of the receiving filter bank convey negligible ISI. The time index i can be dropped for simplicity because the following derivations address the received signals on a symbol-by-symbol basis and the ISI is considered to be negligible. Using Equations 3, 4 and 5, the sampled output of the kth receiving MF can be written as

$$\begin{aligned} Y_k &= \left(r * q_k\right)(t)\Big|_{t=T_{sym}} \\ &= \int_{-\infty}^{\infty} r(\varsigma) q_k\left(T_{sym} - \varsigma\right) d\varsigma \\ &= \int_{T_g}^{T_{sym}} \left(\int_0^{T_g} h(\tau,t)s(\varsigma - \tau)d\tau + w(\varsigma) \right) p_k^*(\varsigma)d\varsigma \\ &= \int_{T_g}^{T_{sym}} \left(\int_0^{T_g} h(\tau,t)\left[\sum_{l=0}^{N-1} X_l p_l(\varsigma - \tau)\right]d\tau \right) p_k^*(\varsigma)d\varsigma + \int_{T_g}^{T_{sym}} w(\varsigma)p_k^*(\varsigma)d\varsigma. \end{aligned} \tag{6}$$

It is assumed that although the CIR is time-varying, it does not significantly change within a few OFDM symbols. Therefore, the CIR can be further represented as $h(\tau)$. Equation 6 can thus be rewritten as

$$Y_k = \sum_{l=0}^{N-1} X_l \int_{T_g}^{T_{sym}} \left(\int_0^{T_g} h(\tau)p_l(\varsigma - \tau)d\tau \right) p_k^*(\varsigma)d\varsigma + \int_{T_g}^{T_{sym}} w(\varsigma)p_k^*(\varsigma)d\varsigma. \tag{7}$$

From Equation 7, if $T_g < \varsigma < T_{sym}$ and $0 < \tau < T_g$, then $0 < \varsigma - \tau < T_{sym}$. Therefore, by substituting Equation 1 into Equation 7, the inner-most integral of Equation 7 can be reformulated as

$$\begin{aligned} \int_0^{T_g} h(\tau)p_l\left(\varsigma - \tau\right)d\tau &= \int_0^{T_g} h(\tau)\frac{e^{j2\pi l(\varsigma - \tau - T_g)B/N}}{\sqrt{T}}d\tau \\ &= \frac{e^{j2\pi l(\varsigma - T_g)B/N}}{\sqrt{T}}\int_0^{T_g} h(\tau)e^{-j2\pi l\tau B/N}d\tau, \quad T_g < \varsigma < T_{sym}. \end{aligned} \tag{8}$$

Furthermore, the integration in Equation 8 can be considered to be the channel weight of the lth sub-channel, whose sub-carrier frequency is $f = lB/N$, i.e.,

$$H_l = H\left(l\frac{B}{N}\right) = \int_0^{T_g} h(\tau)e^{-j2\pi l\tau B/N}d\tau, \tag{9}$$

where $H(f)$ denotes the channel transfer function (CTF) and is thus the Fourier transform of $h(\tau)$. The output of the kth receiving MF can therefore be rewritten as

$$
\begin{aligned}
Y_k &= \sum_{l=0}^{N-1} X_l \int_{T_g}^{T_{sym}} \frac{e^{j2\pi l(\varsigma-T_g)B/N}}{\sqrt{T}} H_l p_k^*(\varsigma)d\varsigma + \int_{T_g}^{T_{sym}} w(\varsigma)p_k^*(\varsigma)d\varsigma \\
&= \sum_{l=0}^{N-1} X_l H_l \int_{T_g}^{T_{sym}} p_l(\varsigma)p_k^*(\varsigma)d\varsigma + W_k,
\end{aligned}
\tag{10}
$$

where

$$
W_k = \int_{T_g}^{T_{sym}} w(\varsigma)p_k^*(\varsigma)d\varsigma.
$$

The transmitting filters $p_k(t)$, $k = 0,1,\cdots,N-1$ employed here are mutually orthogonal, i.e.,

$$
\begin{aligned}
\int_{T_g}^{T_{sym}} p_l(t)p_k^*(t)dt &= \int_{T_g}^{T_{sym}} \frac{e^{j2\pi l(t-T_g)B/N}}{\sqrt{T}}\frac{e^{-j2\pi k(t-T_g)B/N}}{\sqrt{T}}dt \\
&= \delta[k-l],
\end{aligned}
\tag{11}
$$

where

$$
\delta[k-l] = \begin{cases} 1 & k = l \\ 0 & \text{otherwise} \end{cases}
$$

is the Kronecker delta function. Therefore, Equation 10 can be reformulated as

$$
Y_k = H_k X_k + W_k, \qquad k = 0,1,\cdots,N-1,
\tag{12}
$$

where W_k is the AWGN of the kth sub-channel. As a result, the OFDM communication system can be considered to be a set of parallel frequency-flat (frequency-nonselective) fading sub-channels with uncorrelated noise, as depicted in Fig. 3.
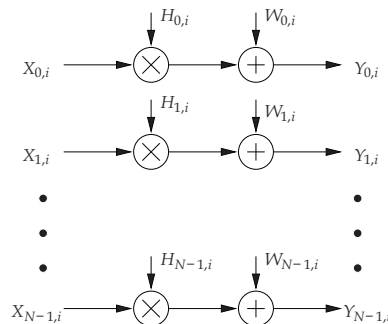

Fig. 3. OFDM communication is converted to transmission over parallel frequency-flat sub-channels.

1.5.2 Discrete-time model

A fully discrete-time representation of the OFDM communication system studied here is depicted in Fig. 4. The modulation and demodulation operations in the continuous-time model have been replaced by IDFT and DFT operations, respectively, and the channel has been replaced by a discrete-time channel.
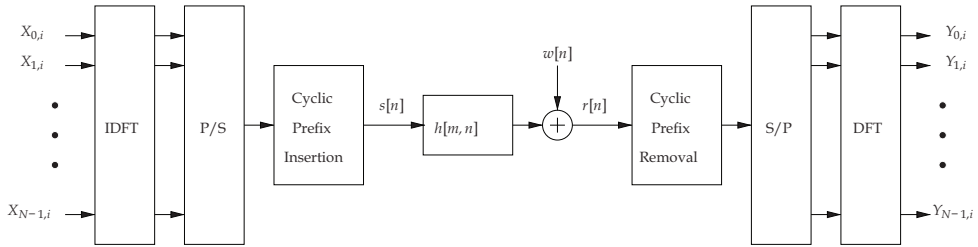

Fig. 4. Discrete-time representation of a base-band equivalent OFDM communication system.

If the CP is longer than the CIR, then the linear convolution operation can be converted to a cyclic convolution. The cyclic convolution is denoted as '⊗' in this chapter. The ith block of the received signals can be written as

$$\begin{aligned} \mathbf{Y}_i &= \mathrm{DFT}_N\left\{\mathrm{IDFT}_N\{\mathbf{X}_i\} \otimes \mathbf{h}_i + \mathbf{w}_i\right\} \\ &= \mathrm{DFT}_N\left\{\mathrm{IDFT}_N\{\mathbf{X}_i\} \otimes \mathbf{h}_i\right\} + \mathbf{W}_i, \end{aligned} \tag{13}$$

where $\mathbf{Y}_i = [Y_{0,i}\ Y_{1,i}\ \cdots\ Y_{N-1,i}]^T$ is an $N \times 1$ vector, and its elements represent N demodulated symbols; $\mathbf{X}_i = [X_{0,i}\ X_{1,i}\ \cdots\ X_{N-1,i}]^T$ is an $N \times 1$ vector, and its elements represent N transmitted information-bearing symbols; $\mathbf{h}_i = [h_{0,i}\ h_{1,i}\ \cdots\ h_{N-1,i}]^T$ is an $N \times 1$ vector, and its elements represent the CIR padded with sufficient zeros to have N dimensions; and $\mathbf{w}_i = [w_{0,i}\ w_{1,i}\ \cdots\ w_{N-1,i}]^T$ is an $N \times 1$ vector representing noise. Because the noise is assumed to be white, Gaussian and circularly symmetric, the noise term

$$\mathbf{W}_i = \mathrm{DFT}_N(\mathbf{w}_i) \tag{14}$$

represents uncorrelated Gaussian noise, and $W_{k,i}$ and $w_{n,i}$ can be proven to have the same variance according to the Central Limit Theorem (CLT). Furthermore, if a new operator "⊙" is defined to be element-by-element multiplication, Equation 13 can be rewritten as

$$\begin{aligned} \mathbf{Y}_i &= \mathbf{X}_i \odot \mathrm{DFT}_N\{\mathbf{h}_i\} + \mathbf{W}_i \\ &= \mathbf{X}_i \odot \mathbf{H}_i + \mathbf{W}_i, \end{aligned} \tag{15}$$

where $\mathbf{H}_i = \mathrm{DFT}_N\{\mathbf{h}_i\}$ is the CTF. As a result, the same set of parallel frequency-flat sub-channels with noise as presented in the continuous-time model can be obtained.

Both the aforementioned continuous-time and discrete-time representations provide insight and serve the purpose of providing a friendly first step or entrance point for beginning readers. In my personal opinion, researchers that have more experience in communication fields may be more comfortable with the continuous-time model because summations, integrations and convolutions are employed in the modulation, demodulation and (CIR)

filtering processes. Meanwhile, researchers that have more experience in signal processing fields may be more comfortable with the discrete-time model because vector and matrix operations are employed in the modulation, demodulation and (CIR) filtering processes. Although the discrete-time model may look neat, clear and reader-friendly, several presumptions should be noted and kept in mind. It is assumed that the symbol shaping is rectangular and that the frequency offset, ISI and ICI are negligible. The primary goal of this chapter is to highlight concepts and provide insight to beginning researchers and practical engineers rather than covering theories or theorems. As a result, the derivations shown in Sections 3 and 4 are close to the continuous-time representation, and those in Sections 5 and 6 are derived from the discrete-time representation.

2. Introduction to channel estimation on wireless OFDM communications

2.1 Preliminary

In practice, effective channel estimation (CE) techniques for coherent OFDM communications are highly desired for demodulating or detecting received signals, improving system performance and tracking time-varying multipath channels, especially for mobile OFDM because these techniques often operate in environments where signal reception is inevitably accompanied by wide Doppler spreads caused by dynamic surroundings and long multipath delay spreads caused by time-dispersion. Significant research efforts have focused on addressing various CE and subsequent equalization problems by estimating sub-channel gains or the CIR. CE techniques in OFDM systems often exploit several pilot symbols transceived at given locations on the frequency-time grid to determine the relevant channel parameters. Several previous studies have investigated the performance of CE techniques assisted by various allocation patterns of the pilot/training symbols (Coleri et al., 2002; Li et al., 2002; Yeh & Lin, 1999; Negi & Cioffi, 1998). Meanwhile, several prior CEs have simultaneously exploited both time-directional and frequency-directional correlations in the channel under investigation (Hoeher et al., 1997; Wilson et al., 1994; Hoeher, 1991). In practice, these two-dimensional (2D) estimators require 2D Wiener filters and are often too complicated to be implemented. Moreover, it is difficult to achieve any improvements by using a 2D estimator, while significant computational complexity is added (Sandell & Edfors, 1996). As a result, serially exploiting the correlation properties in the time and frequency directions may be preferred (Hoeher, 1991) for reduced complexity and good estimation performance. In mobile environments, channel tap-weighting coefficients often change rapidly. Thus, the comb-type pilot pattern, in which pilot symbols are inserted and continuously transmitted over specific pilot sub-channels in all OFDM blocks, is naturally preferred and highly desirable for effectively and accurately tracking channel time-variations (Negi & Cioffi, 1998; Wilson et al., 1994; Hoeher, 1991; Hsieh & Wei, 1998).

Several methods for allocating pilots on the time-frequency grid have been studied (Tufvesson & Maseng, 1997). Two primary pilot assignments are depicted in Fig. 5: the block-type pilot arrangement (BTPA), shown in Fig. 5(a), and the comb-type pilot arrangement (CTPA), shown in Fig. 5(b). In the BTPA, pilot signals are assigned in specific OFDM blocks to occupy all sub-channels and are transmitted periodically. Both in general and in theory, BTPA is more suitable in a slowly time-varying, but severely frequency-selective fading environment. No interpolation method in the FD is required because the pilot block occupies the whole band. As a result, the BTPA is relatively insensitive to severe

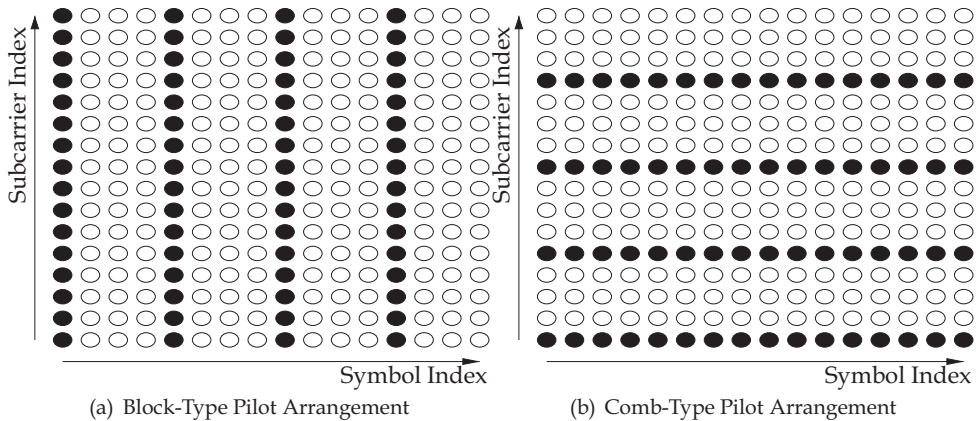(a) Block-Type Pilot Arrangement   (b) Comb-Type Pilot Arrangement

Fig. 5. Two primary pilot assignment methods

frequency selectivity in a multipath fading channel. Estimates of the CIR can usually be obtained by least-squares (LS) or minimum-mean-square-error (MMSE) estimations conducted with assistance from the pilot symbols (Edfors et al., 1996; Van de Beek et al., 1995).

In the CTPA, pilot symbols are often uniformly distributed over all sub-channels in each OFDM symbol. Therefore, the CTPA can provide better resistance to channel time-variations. Channel weights on non-pilot (data) sub-channels have to be estimated by interpolating or smoothing the estimates of the channel weights obtained on the pilot sub-channels (Zhao & Huang, 1997; Rinne & Renfors, 1996). Therefore, the CTPA is, both in general and in theory, sensitive to the frequency-selectivity of a multipath fading channel. The CTPA is adopted to assist the CE conducted in each OFDM block in Sections 3 and 4, while the BTPA is discussed in Section 5.

2.2 CTPA-based CE

Conventional CEs assisted by comb-type pilot sub-channels are often performed completely in the frequency domain (FD) and include two steps: jointly estimating the channel gains on all pilot sub-channels and smoothing the obtained estimates to interpolate the channel gains on data (non-pilot) sub-channels. The CTPA CE technique (Hsieh & Wei, 1998) and the pilot-symbol-assisted modulation (PSAM) CE technique (Edfors et al., 1998) have been shown to be practical and applicable methods for mobile OFDM communication because their ability to track rapidly time-varying channels is much better than that of a BTPA CE technique. Several modified variants for further improvements and for complexity or rank reduction by means of singular-value-decomposition (SVD) techniques have been investigated previously (Hsieh & Wei, 1998; Edfors et al., 1998; Seller, 2004; Edfors et al., 1996; Van de Beek et al., 1995; Park et al., 2004). In addition, a more recent study has proposed improving CE performance by taking advantage of presumed slowly varying properties in the delay subspace (Simeone et al., 2004). This technique employs an intermediate step between the LS pilot sub-channel estimation step and the data sub-channel interpolation step in conventional CE approaches (Hsieh & Wei, 1998; Edfors et al., 1998; Seller, 2004; Edfors et al., 1996; Van de Beek et al., 1995; Park et al., 2004) to track the delay subspace to improve the accuracy of the pilot sub-channel estimation. However, this

technique is based on the strong assumption that the multipath delays are slowly time-varying and can easily be estimated separately from the channel gain estimation. A prior channel estimation study (Minn & Bhargava, 2000) also exploited CTPA and TD CE. The proposed technique (Minn & Bhargava, 2000) was called the Frequency-Pilot-Time-Average (FPTA) method. However, time-averaging over a period that may be longer than the coherence time of wireless channels to suppress interference not only cannot work for wireless applications with real-time requirements but may also be impractical in a mobile channel with a short coherence time. A very successful technique that takes advantage of TD CE has been proposed (Minn & Bhargava, 1999). However, this technique focused on parameter estimation to transmit diversity using space-time coding in OFDM systems, and the parameter settings were not obtained from any recent mobile communication standards. To make fair comparisons of the CE performance and to avoid various diversity or space-time coding methods, only uncoded OFDM with no diversity is addressed in this chapter.

The CTPA is also employed as the framework of the technique studied in Sections 3 and 4 because of its effectiveness in mobile OFDM communications with rapidly time-varying, frequency-selective fading channels. A least-squares estimation (LSE) approach is performed serially on a block-by-block basis in the TD, not only to accurately estimate the CIR but also to effectively track rapid CIR variations. In fact, a generic estimator is thus executed on each OFDM block without assistance from a priori channel information (e.g., correlation functions in the frequency and/or in the time directions) and without increasing computational complexity.

Many previous studies (Edfors et al., 1998; Seller, 2004; Edfors et al., 1996; Van de Beek et al., 1995; Simeone et al., 2004) based on CTPA were derived under the assumption of perfect timing synchronization. In practice, some residual timing error within several sampling durations inevitably occurs during DFT demodulation, and this timing error leads to extra phase errors that phase-rotate demodulated symbols. Although a method that solves this problem in conventional CTPA OFDM CEs has been studied (Hsieh & Wei, 1998; Park et al., 2004), this method can work only under some special conditions (Hsieh & Wei, 1998). Compared with previous studies (Edfors et al., 1998; Seller, 2004; Edfors et al., 1996; Van de Beek et al., 1995; Simeone et al., 2004), the studied technique can be shown to achieve better resistance to residual timing errors because it does not employ a priori channel information and thus avoids the model mismatch and extra phase rotation problems that result from residual timing errors. Also, because the studied technique performs ideal data sub-channel interpolation with a domain-transformation approach, it can effectively track extra phase rotations with no phase lag.

2.3 BTPA-based CE

Single-carrier frequency-division multiple-access (SC-FDMA) communication was selected for the long-term evolution (LTE) specification in the third-generation partnership project (3GPP). SC-FDMA has been the focus of research and development because of its ability to maintain a low peak-to-average power ratio (PAPR), particularly in the uplink transmission, which is one of a few problems in recent 4G mobile communication standardization. Meanwhile, SC-FDMA can maintain high throughput and low equalization complexity like orthogonal frequency-division multiple access (OFDMA) (Myung et al., 2006). Moreover, SC-FDMA can be thought of as an OFDMA with DFT pre-coded or pre-spread inputs. In a SC-FDMA uplink scenario, information-bearing symbols in the TD from any individual user terminal are pre-coded (or pre-spread) with a DFT. The DFT-spread resultant symbols can

be transformed into the FD. Finally, the DFT-spread symbols are fed into an IDFT multiplexer to accomplish FDM.

Although the CTPA is commonly adopted in wireless communication applications, such as IEEE 802.11a, IEEE 802.11g, IEEE 802.16e and the EU-IST-4MORE project, the BTPA is employed in the LTE. As shown in the LTE specification, 7 symbols form a slot, and 20 slots form a frame that spans 10 ms in the LTE uplink transmission. In each slot, the 4th symbol is used to transmit a pilot symbol. Section 5 employs BTPA as the framework to completely follow the LTE specifications. A modified Kalman filter- (MKF-) based TD CE approach with fast fading channels has been proposed previously (Han et al., 2004). The MKF-based TD CE tracks channel variations by taking advantage of MKF and TD MMSE equalizers. A CE technique that also employs a Kalman filter has been proposed (Li et al., 2008). Both methods successfully address the CE with high Doppler spreads.

The demodulation reference signal adopted for CE in LTE uplink communication is generated from Zadoff-Chu (ZC) sequences. ZC sequences, which are generalized chirp-like poly-phase sequences, have some beneficial properties according to previous studies (Ng et al., 1998; Popovic, 1992). ZC sequences are also commonly used in radar applications and as synchronization signals in LTE, e.g., random access and cell search (Levanon & Mozeson, 2004; LTE, 2009). A BTPA-based CE technique is discussed in great detail in Section 5.

2.4 TD-redundancy-based CE

Although the mobile communication applications mentioned above are all based on cyclic-prefix OFDM (CP-OFDM) modulation techniques, several encouraging contributions have investigated some alternatives, e.g., zero-padded OFDM (ZP-OFDM) (Muquest et al., 2002; Muquet et al., 2000) and pseudo-random-postfix OFDM (PRP-OFDM) (Muck et al., 2006; 2005; 2003) to replace the TD redundancy with null samples or known/pre-determined sequences. It has been found that significant improvements over CP-OFDM can be realized with either ZP-OFDM or PRP-OFDM (Muquest et al., 2002; Muquet et al., 2000; Muck et al., 2006; 2005; 2003). In previous works, ZP-OFDM has been shown to maintain symbol recovery irrespective of null locations on a multipath channel (Muquest et al., 2002; Muquet et al., 2000). Meanwhile, PRP-OFDM replaces the null samples originally inserted between any two OFDM blocks in ZP-OFDM by a known sequence. Thus, the receiver can use the a priori knowledge of a fraction of transmitted blocks to accurately estimate the CIR and effectively reduce the loss of transmission rate with frequent, periodic training sequences (Muck et al., 2006; 2005; 2003). A more recent OFDM variant, called Time-Domain Synchronous OFDM (TDS-OFDM) was investigated in terrestrial broadcasting applications (Gui et al., 2009; Yang et al., 2008; Zheng & Sun, 2008; Liu & Zhang, 2007; Song et al., 2005). TDS-OFDM works similarly to the PRP-OFDM and also belongs to this category of CEs assisted by TD redundancy.

Several research efforts that address various PRP-OFDM CE and/or subsequent equalization problems have been undertaken (Muck et al., 2006; 2005; 2003; Ma et al., 2006). However, these studies were performed only in the context of a wireless local area network (WLAN), in which multipath fading and Doppler effects are not as severe as in mobile communication. In addition, the techniques studied in previous works (Muck et al., 2006; 2005; 2003; Ma et al., 2006) take advantage of a time-averaging method to replace statistical expectation operations and to suppress various kinds of interference, including inter-block interference (IBI) and ISI. However, these moving-average-based interference suppression methods investigated in the previous studies (Muck et al., 2006; 2005; 2003; Ma et al., 2006)

cannot function in the mobile environment because of rapid channel variation and real-time requirements. In fact, it is difficult to design an effective moving-average filter (or an integrate-and-dump (I/D) filter) for the previous studies (Muck et al., 2006; 2005; 2003; Ma et al., 2006) because the moving-average filter must have a sufficiently short time-averaging duration (i.e., sufficiently short I/D filter impulse response) to accommodate both the time-variant behaviors of channel tap-weighting coefficients and to keep the a priori statistics of the PRP unchanged for effective CE and must also have a sufficiently long time-averaging duration (i.e., sufficiently long I/D filter impulse response) to effectively suppress various kinds of interference and reduce AWGN.

A previous work (Ohno & Giannakis, 2002) investigated an optimum training pattern for generic block transmission over time-frequency selective channels. It has been proven that the TD training sequences must be placed with equal spacing to minimize mean-square errors. However, the work (Ohno & Giannakis, 2002) was still in the context of WLAN and broadcasting applications, and no symbol recovery method was studied. As shown in Section 6, the self-interference that occurs with symbol recovery and signal detection must be further eliminated by means of the SIC method.

3. Frequency-domain channel estimation based on comb-type pilot arrangement

3.1 System description

The block diagram of the OFDM transceiver under study is depicted in Fig. 6. Information-bearing bits are grouped and mapped according to Gray encoding to become multi-amplitude-multi-phase symbols. After pilot symbol insertion, the block of data $\{X_k, k = 0, 1, \cdots, N-1\}$ is then fed into the IDFT (or IFFT) modulator. Thus, the modulated symbols $\{x_n, n = 0, 1, \cdots, N-1\}$ can be expressed as

$$x_n = \frac{1}{\sqrt{N}} \sum_{k=0}^{N-1} X_k e^{j2\pi kn/N}, \quad n = 0, 1, \cdots, N-1, \tag{16}$$

where N is the number of sub-channels. In the above equation, it is assumed that there are no virtual sub-carriers, which provide guard bands, in the studied OFDM system. A CP is arranged in front of an OFDM symbol to avoid ISI and ICI, and the resultant symbol $\{x_{cp,n}, n = -L, -L+1, \cdots, N-1\}$ can thus be expressed as

$$x_{cp,n} = \begin{cases} x_{N+n} & n = -L, -L+1, \cdots, -1 \\ x_n & n = 0, 1, \cdots, N-1, \end{cases} \tag{17}$$

where L denotes the number of CP samples. The transmitted signal is then fed into a multipath fading channel with CIR $h[m,n]$. The received signal can thus be represented as

$$y_{cp}[n] = x_{cp}[n] \otimes h[m,n] + w[n], \tag{18}$$

where $w[n]$ denotes the AWGN. The CIR $h[m,n]$ can be expressed as (Steele, 1999)

$$h[m,n] = \sum_{i=0}^{M-1} \alpha_i e^{j2\pi v_i n T_s} \delta[m T_s - \tau_i], \tag{19}$$

where M denotes the number of resolvable propagation paths, α_i represents the ith complex channel weight of the CIR, ν_i denotes the maximum Doppler frequency on the ith resolvable propagation path, m is the index in the delay domain, n is the time index, and τ_i denotes the delay of the ith resolvable path.
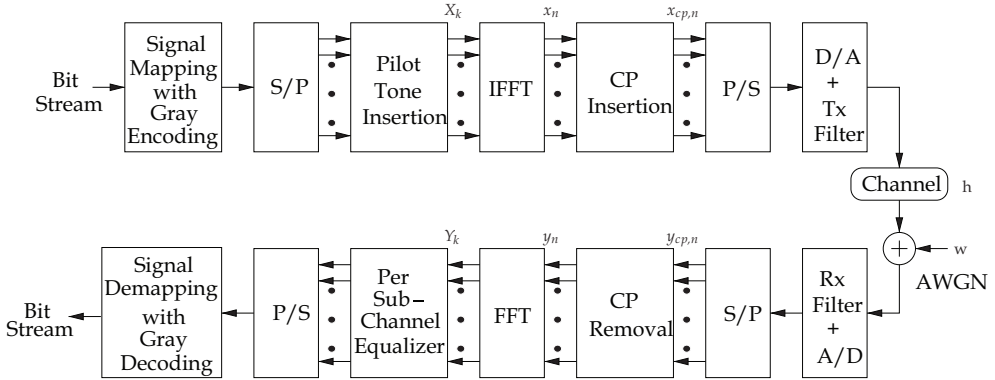

Fig. 6. A base-band equivalent block diagram of the studied OFDM transceiver.

After the CP portion is effectively removed from $y_{cp,n}$, the received samples y_n are sifted and fed into the DFT demodulator to simultaneously demodulate the signals propagating through the multiple sub-channels. The demodulated symbol obtained on the kth sub-channel can thus be written as

$$Y_k = \frac{1}{\sqrt{N}} \sum_{n=0}^{N-1} y_n e^{-j2\pi kn/N}, \qquad k = 0, 1, \cdots, N-1. \tag{20}$$

If the CP is sufficiently longer than the CIR, then the ISI among OFDM symbols can be neglected. Therefore, Y_k can be reformulated as (Zhao & Huang, 1997; Hsieh & Wei, 1998)

$$Y_k = X_k H_k + I_k + W_k, \qquad k = 0, 1, \cdots, N-1, \tag{21}$$

where

$$
\begin{aligned}
H_k &= \sqrt{N} \sum_{i=0}^{M-1} \alpha_i e^{j\pi \nu_i T} \frac{\sin(\pi \nu_i T)}{\pi \nu_i T} e^{-j\frac{2\pi \tau_i}{N}k}, \\
I_k &= \frac{1}{\sqrt{N}} \sum_{i=0}^{M-1} \alpha_i \sum_{\substack{k'=0 \\ k' \neq k}}^{N-1} X(k') \frac{1 - e^{j2\pi(\nu_i T + k' - k)}}{1 - e^{j\frac{2\pi}{N}(\nu_i T + k' - k)}} e^{-j\frac{2\pi \tau_i}{N}k'}, \qquad k = 0, 1, \cdots, N-1
\end{aligned}
\tag{22}
$$

and $\{W_k, k = 0, 1, \cdots, N-1\}$ is the Fourier transform of $\{w_n, n = 0, 1, \cdots, N-1\}$.

The symbols $\{Y_{p,k}\}$ received on the pilot sub-channels can be obtained from $\{Y_k, k = 0, 1, \cdots, N-1\}$, the channel weights on the pilot sub-channels $\{H_{p,k}\}$ can be estimated, and then the channel weights on the data (non-pilot) sub-channels can be obtained by interpolating or smoothing the obtained estimates of the pilot sub-channel weights $H_{p,k}$. The transmitted information-bearing symbols $\{X_k, k=0, 1, \cdots, N-1\}$ can be recovered by simply dividing the received symbols by the corresponding channel weights, i.e.,

$$\hat{X}_k = \frac{Y_k}{\hat{H}_k}, \qquad k = 0,1,\cdots,N-1, \tag{22}$$

where $\hat{H}_k$ is an estimate of H_k. Eventually, the source binary data may be reconstructed by means of signal demapping.

3.2 Pilot sub-channel estimation

In the CTPA, the N_p pilot signals $X_{p,m}$, $m = 0,1, \cdots,N_p - 1$ are inserted into the FD transmitted symbols X_k, $k = 0,1, \cdots,N - 1$ with equal separation. In other words, the total N sub-carriers are divided into N_p groups, each of which contains $Q = N/N_p$ contiguous sub-carriers. Within any group of sub-carriers, the first sub-carrier, with the lowest central frequency, is adopted to transmit pilot signals. The value of $\rho = Q^{-1}$ denotes the pilot density employed in the OFDM communication studied here. The pilot density ρ represents the portion of the entire bandwidth that is employed to transmit the pilots, and it must be as low as possible to maintain sufficiently high bandwidth efficiency. However, the Nyquist sampling criterion sets a lower bound on the pilot density ρ that allows the CTF to be effectively reconstructed with a subcarrier-domain (i.e., FD) interpolation approach. The OFDM symbol transmitted over the kth sub-channel can thus be expressed as

$$\begin{aligned} X_k \quad &= X_{mQ+l} \\ &= \begin{cases} X_{p,m'} & l = 0, \\ \text{information,} & l = 1,2,\cdots,Q-1. \end{cases} \end{aligned} \tag{23}$$

The pilot signals $\{X_{p,m}, m = 0, 1, \cdots, N_p - 1\}$ can either be a common complex value or sifted from a pseudo-random sequence.

The channel weights on the pilot sub-channels can be written in vector form, i.e.,

$$\begin{aligned} \mathbf{H}_p \quad &= \begin{bmatrix} H_p(0) & H_p(1) & \cdots & H_p(N_p - 1) \end{bmatrix}^T \\ &= \begin{bmatrix} H(0) & H(Q) & \cdots & H\big((N_p - 1)Q\big) \end{bmatrix}^T. \end{aligned} \tag{24}$$

The received symbols on the pilot sub-channels obtained after the FFT demodulation can be expressed as

$$\mathbf{Y}_p = \begin{bmatrix} Y_{p,0} & Y_{p,1} & \cdots & Y_{p,N_p-1} \end{bmatrix}^T. \tag{25}$$

Moreover, $\mathbf{Y}_p$ can be rewritten as

$$\mathbf{Y}_p = \mathbf{X}_p \cdot \mathbf{H}_p + \mathbf{I}_p + \mathbf{W}_p, \tag{26}$$

where

$$\mathbf{X}_p = \begin{bmatrix} X_p(0) & & \mathbf{0} \\ & \ddots & \\ \mathbf{0} & & X_p(N_p - 1) \end{bmatrix},$$

$\mathbf{I}_p$ denotes the ICI vector and $\mathbf{W}_p$ denotes the AWGN of the pilot sub-channels.

In conventional CTPA-based CE methods, the estimates of the channel weights of the pilot sub-channels can be obtained by means of the LS CE, i.e.,

$$
\begin{aligned}
\widehat{\mathbf{H}}_{LS} \quad &= \begin{bmatrix} H_{p,LS}(0) & H_{p,LS}(1) & \cdots & H_{p,LS}(N_p-1) \end{bmatrix}^T \\
&= \left(\mathbf{X}_p^H \mathbf{X}_p \right)^{-1} \mathbf{X}_p^H \mathbf{Y}_p = \mathbf{X}_p^{-1} \mathbf{Y}_p \\
&= \begin{bmatrix} \dfrac{Y_p(0)}{X_p(0)} & \dfrac{Y_p(1)}{X_p(1)} & \cdots & \dfrac{Y_p(N_p-1)}{X_p(N_p-1)} \end{bmatrix}^T .
\end{aligned}
\tag{27}
$$

Although the aforementioned LS CE $\widehat{\mathbf{H}}_{LS}$ enjoys low computational complexity, it suffers from noise enhancement problems, like the zero-forcing equalizer discussed in textbooks.

The MMSE criterion is adopted in CE and equalization techniques, and it exhibits better CE performance than the LS CE in OFDM communications assisted by block pilots (Van de Beek et al., 1995). The main drawback of the MMSE CE is its high complexity, which grows exponentially with the size of the observation samples. In a previous study (Edfors et al., 1996), a low-rank approximation was applied to a linear minimum-mean-square-error (LMMSE) CE assisted by FD correlation. The key idea to reduce the complexity is using the singular-value-decomposition (SVD) technique to derive an optimal low-rank estimation, the performance of which remains essentially unchanged. The MMSE CE performed on the pilot sub-channels is formulated as follows (Edfors et al., 1996):

$$
\begin{aligned}
\widehat{\mathbf{H}}_{LMMSE} \quad &= \mathbf{R}_{\hat{H}_{LS}\hat{H}_{LS}} \mathbf{R}_{H_p\hat{H}_{LS}}^{-1} \widehat{\mathbf{H}}_{LS} \\
&= \mathbf{R}_{H_pH_p} \left(\mathbf{R}_{H_pH_p} + \sigma_w^2 \left(\mathbf{X}_p \mathbf{X}_p^H \right)^{-1} \right)^{-1} \widehat{\mathbf{H}}_{LS},
\end{aligned}
\tag{28}
$$

where $\widehat{\mathbf{H}}_{LS}$ is the LS estimate of $\mathbf{H}_p$ derived in Equation 27, σ_w^2 is the common variance of W_k and w_n, and the covariance matrices are defined as follows:

$$
\begin{aligned}
\mathbf{R}_{H_pH_p} \quad &= E\left\{ \mathbf{H}_p \mathbf{H}_p^H \right\}, \\
\mathbf{R}_{H_p\hat{H}_{LS}} \quad &= E\left\{ \mathbf{H}_p \widehat{\mathbf{H}}_{LS}^H \right\}, \\
\mathbf{R}_{\hat{H}_{LS}\hat{H}_{LS}} \quad &= E\left\{ \widehat{\mathbf{H}}_{LS} \widehat{\mathbf{H}}_{LS}^H \right\}.
\end{aligned}
$$

It is observed from Equation 28 that a matrix inversion operation is involved in the MMSE estimator, and it must be calculated symbol by symbol. This problem can be solved by using a constant pilot, e.g., $X_{p,m} = c$, $m = 0, 1, \cdots, N_p - 1$. A generic CE can be obtained by averaging over a sufficiently long duration of transmitted symbols (Edfors et al., 1996), i.e.,

$$
\widehat{\mathbf{H}}_{LMMSE} = \mathbf{R}_{H_pH_p} \left(\mathbf{R}_{H_pH_p} + \frac{\beta}{\Gamma} \mathbf{I} \right)^{-1} \widehat{\mathbf{H}}_{LS},
\tag{29}
$$

where $\Gamma = \dfrac{\mathrm{E}\{|X_{p,k}|^2\}}{\sigma_w^2}$ is the average signal-to-noise ratio (SNR) and $\beta =$
$\mathrm{E}\{|X_{p,k}|^2\}\mathrm{E}\{|1/X_{p,k}|^2\}$ is a constant determined by the signal mapping method employed in the pilot symbols. For example, $\beta = 17/9$ if 16-QAM is employed in the pilot symbols. If the auto-correlation matrix $\mathbf{R}_{H_p H_p}$ and the value of the SNR are known in advance,

$\mathbf{R}_{H_p H_p}\left(\mathbf{R}_{H_p H_p}+\dfrac{\beta}{\Gamma}\mathbf{I}\right)^{-1}$ only needs to be calculated once. As shown in Equation 29, the CE
requires N_p complex multiplications per pilot sub-carrier. To further reduce the number of multiplication operations, a low-rank approximation method based on singular-value decomposition (SVD) was adopted in the previous study (Edfors et al., 1996). Initially, the channel correlation matrix can be decomposed as

$$\mathbf{R}_{H_p H_p} = \mathbf{U}\boldsymbol{\Lambda}\mathbf{U}^H,\tag{30}$$

where $\mathbf{U}$ is a matrix with orthonormal columns $\mathbf{u}_0,\mathbf{u}_1,\cdots,\mathbf{u}_{N_p-1}$, and $\boldsymbol{\Lambda}$ is a diagonal matrix with singular values $\lambda_0,\lambda_1,\cdots,\lambda_{N_p-1}$ as its diagonal elements. The rank-ϱ approximation of the LMMSE CE derived in Equation 29 can thus be formulated as

$$\widehat{\mathbf{H}}_{SVD} = \mathbf{U}\begin{bmatrix}\boldsymbol{\Delta}_\varrho & 0\\ 0 & 0\end{bmatrix}\mathbf{U}^H\widehat{\mathbf{H}}_{LS},\tag{31}$$

where $\boldsymbol{\Delta}_\varrho$ denotes a diagonal matrix with terms that can be expressed as

$$\delta_k = \frac{\lambda_k}{\lambda_k + \dfrac{\beta}{\Gamma}},\qquad k = 0,1,\cdots,\varrho.\tag{32}$$

After some manipulation, the CE in Equation 31 requires $2\varrho N_p$ complex multiplications, and the total number of multiplications per pilot tone becomes 2ϱ. In general, the number of essential singular values, ϱ, is much smaller than the number of pilot sub-channels, N_p, and the computational complexity is therefore considerably reduced when the low-rank SVD-based CE is compared with the full-rank LMMSE-based CE derived in Equation 29. Incidentally, low-rank SVD-based CE can combat parameter mismatch problems, as shown in previous studies (Edfors et al., 1996).

3.3 Data sub-channel interpolation
After joint estimation of the FD channel weights from the pilot sub-channels is complete, the channel weight estimation on the data (non-pilot) sub-channels must be interpolated from the pilot sub-channel estimates. A piecewise-linear interpolation method has been studied (Rinne & Renfors, 1996) that exhibits better CE performance than piecewise-constant interpolation. A piecewise-linear interpolation (LI) method, a piecewise second-order polynomial interpolation (SOPI) method and a transform-domain interpolation method are studied in this sub-section.

3.3.1 Linear interpolation

In the linear interpolation method, the channel weight estimates on any two adjacent pilot sub-channels are employed to determine the channel weight estimates of the data sub-channel located between the two pilot sub-channels (Rinne & Renfors, 1996). The channel estimate of the kth data sub-channel can be obtained by the LI method, i.e.,

$$\hat{H}_{LI,x,k} = \hat{H}_{LI,x,mQ+l} = \left(1 - \frac{l}{Q}\right)\hat{H}_{x,m} + \frac{l}{Q}\hat{H}_{x,m+1}, \quad \begin{array}{l} x = LS, LMMSE, SVD, \\ m = 0, 1, \cdots, N_p - 2, \\ 1 \le l \le (Q-1), \end{array} \tag{33}$$

where $mQ < k = mQ + l < (m+1)Q$, $m = \lfloor \frac{k}{Q} \rfloor$, $\lfloor \cdot \rfloor$ denotes the greatest integer less than or equal to the argument and l is the value of k modulo Q.

3.3.2 Second-order polynomial interpolation

Intuitively, a higher-order polynomial interpolation may fit the CTF better than the aforementioned first-order polynomial interpolation (LI). The SOPI can be implemented with a linear, time-invariant FIR filter (Liu & Wei, 1992), and the interpolation can be written as

$$\begin{aligned} \hat{H}_{SOPI,k} &= \hat{H}_{SOPI,x,mQ+l} \\ &= c_1 \hat{H}_{x,m-1} + c_0 \hat{H}_{x,m} + c_{-1}\hat{H}_{x,m+1}, \end{aligned} \tag{34}$$

where

$$x = LS, LMMSE, SVD, \qquad m = 1, 2 \cdots, N_p - 2, \qquad 1 \le l \le (Q-1),$$

$$c_1 = \frac{\psi(\psi+1)}{2}, \qquad c_0 = -(\psi-1)(\psi+1), \qquad c_{-1} = \frac{\psi(\psi-1)}{2},$$

$$\psi = \frac{l}{N}.$$

3.3.3 Transform-domain-processing-based interpolation (TFDI)

An ideal low-pass filtering method based on transform-domain processing was adopted for the data sub-channel interpolation (Zhao & Huang, 1997). In accordance with the CTPA, the pilot sub-channels are equally spaced every Q sub-channels. This implies that the coherence bandwidth of the multipath fading channel under consideration is sufficiently wider than the bandwidth occupied by Q sub-channels. After the pilot sub-channel estimation was completed, the interpolation methods mentioned in 3.3.2 and 3.3.3 were used to search for some low-order-polynomial-based estimations (say, LI and SOPI) of the channel weights of the data sub-channels. A transform-domain-processing-based interpolation (TFDI) method proposed in a previous study was used to jointly smooth/filter out the sub-channel weight estimates of the data sub-channels (Zhao & Huang, 1997). The TFDI method consists of the following steps: (1) first, it transforms the sub-channel weight estimates obtained from the pilot sub-channels into the transform domain, which can be thought of as the TD here; (2) it keeps the essential elements unchanged, which include at most the leading N_p (multipath) components because the coherence bandwidth is as wide as N/N_p sub-channels; (3) it sets the tail $(N - N_p)$ components to zero; and (4) finally, it performs the inverse transformation

back to the sub-carrier domain, which may be called the FD in other publications. In this approach, a high-resolution interpolation method based on zero-padding and DFT/IDFT (Elliott, 1988) is employed. The TFDI technique can be thought of as ideal interpolation using an ideal lowpass filter in the transform domain.

3.4 Remarks

In this section, FD CE techniques based on CTPA were studied. Pilot sub-channel estimation techniques based on LS, LMMSE and SVD methods were studied along with data sub-channel interpolation techniques based on LI, SOPI and TFDI. The material provided in this section may also be found in greater detail in many prior publications (cited in this section) for interested readers. Of course, this author strongly encourages potential readers to delve into relevant research.

Many previous studies, e.g., (Zhao & Huang, 1997; Hsieh & Wei, 1998), prefer to adopt the IDFT as $\sum_{k=0}^{N-1} X_k e^{j2\pi kn/N}$ and the DFT as $\frac{1}{N}\sum_{k=0}^{N-1} x_n e^{j2\pi kn/N}$, rather than adopt those written in Equations 16 and 20. Although these representations are equivalent from the viewpoint of signal power, the formulations in Equations 16 and 20 are definitely more effective and convenient because they can keep the post-DFT-demodulation noise variance the same as the pre-DFT-demodulation noise variance. While performance analysis or comparison is conducted in terms of SNR, readers should be noted to take much care on this issue.

4. Time-domain channel estimation based on least-squares technique

4.1 Preliminary

A LS CE technique for mobile OFDM communication over a rapidly time-varying frequency-selective fading channel is demonstrated in this section. The studied technique, which uses CTPA, achieves low error probabilities by accurately estimating the CIR and effectively tracking rapid CIR time-variations. Unlike the technique studied in Section 3, the LS CE technique studied in this section is conducted in the TD, and several virtual sub-carriers are used. A generic estimator is performed serially block by block without assistance from a priori channel information and without increasing the computational complexity. The technique investigated in this section is also resistant to residual timing errors that occur during DFT demodulation. The material studied in this section has been thoroughly documented in a previous study and its references (Lin, 2008c). The author strongly encourages interested readers to look at these previous publications to achieve a deeper and more complete understanding of the material.

4.2 System description

The base-band signal $\{x_n\}$ consists of $2K$ complex sinusoids, which are individually modulated by $2K$ complex information-bearing QPSK symbols $\{X_k\}$, i.e.,

$$x_n = \frac{1}{\sqrt{N}} \sum_{k=-K}^{K-1} X_{|k|_N} e^{j2\pi nk/N}, \qquad n = 0,1,\cdots,N-1, \qquad N \geq 2K, \qquad (35)$$

where $X_{|k|_N}$ denotes the complex symbol transmitted on the $|k|_N$th sub-channel, N is the IDFT size, n is the TD symbol index, k is the FD subcarrier index, $2K$ is the total number of

sub-channels used to transmit information and $|k|_N$ denotes the value of k modulo N. In Equation 35, $N_v = N - 2K$ sub-carriers are appended in the high-frequency bands as virtual sub-carriers and can be considered to be guard bands that avoid interference from other applications in adjacent bands and are not employed to deliver any information. It should be noted that x_n and X_k form an N-point DFT pair, i.e., $\text{DFT}_N \{x_n, n = 0,1, \cdots, N-1\} = \{X_0, X_1, \cdots, X_{K-1}, 0, 0, \cdots, 0, X_{N-K}, X_{N-K+1}, \cdots, X_{N-1}\}$, where the 0s denote the symbols transmitted via the virtual sub-channels. In a CTPA OFDM system, the symbols transmitted on the sub-channels can be expressed in vector form for simplicity:

$$\mathbf{X} = \{X_k\} \in \mathbf{C}^{N \times 1}, \tag{36}$$

where

$$X_k = \begin{cases} 0, & k \in \zeta_v = \{K, K+1, \cdots, N-K-1\} \\ P_l, & k \in \zeta_p = \{|(N-K)+(Q+1)/2 + l \cdot Q|_N| \, l = 0,1,\cdots, N_p - 1\} \\ D_{k'}, & k \in \zeta \setminus \zeta_v \setminus \zeta_p; \end{cases}$$

$\zeta = \{0,1, \cdots, N-1\}$; $K = (N - N_v)/2$; P_l denotes the lth pilot symbol; N_p denotes the number of pilot sub-channels; Q denotes the pilot sub-channel separation, which is an odd number in the case under study; $D_{k'}$ represents the k'th information-bearing data symbol; ζ_v stands for the set of indices of the virtual sub-channels; and ζ_p stands for the set of indices of the pilot sub-channels. The OFDM block modulation can be reformulated as the following matrix operation:

$$\mathbf{x} = \mathbf{F_I} \cdot \mathbf{X}, \tag{37}$$

where

$$\mathbf{x} = \{x_n\} \in \mathbf{C}^{N \times 1};$$
$$\mathbf{F_I} = \{f_{n,k}\} \in \mathbf{C}^{N \times N},$$
$$f_{n,k} = \frac{1}{\sqrt{N}} \exp\left(j\frac{2\pi kn}{N}\right), \quad 0 \le k \le N-1, \quad 0 \le n \le N-1.$$

$\mathbf{x}$ in Equation 37 can be rewritten as follows:

$$\mathbf{x} = \bar{\mathbf{x}} + \tilde{\mathbf{x}}, \tag{38}$$

where

$$\bar{\mathbf{x}} = \{\bar{x}_n\} \in \mathbf{C}^{N \times 1},$$
$$\bar{x}_n = \frac{1}{\sqrt{N}} \sum_{l=0}^{N_p - 1} P_l \cdot \exp\left(j2\pi n \big|(N-K)+(Q+1)/2 + l \cdot Q\big|_N / N\right),$$
$$n = 0, 1, \cdots, N-1,$$

which is the TD sequence obtained from the pilot symbols modulated on the pilot sub-channels; and

$$\tilde{\mathbf{x}} = \{\tilde{x}_n\} \in \mathbf{C}^{N \times 1},$$

$$\tilde{x}_n = \frac{1}{\sqrt{N}} \sum_{\substack{k=0 \\ k \notin \zeta_v \\ k \notin \zeta_p}}^{N-1} X_k \cdot \exp\left(j2\pi nk / N\right), \qquad n = 0, 1, \cdots, N-1,$$

which is the TD sequence that results from the information-bearing QPSK symbols modulated on the data (non-pilot) sub-channels. In accordance with the CLT, $\tilde{x}_n$, $n = 0, 1, \cdots$, $N - 1$ are independent, identically distributed (IID) zero-mean Gaussian random variables with variance $\frac{N - N_v - N_p}{N} \sigma_{X_k}^2$, where $\sigma_{X_k}^2$ is the transmitted signal power.

After the TD signal $\mathbf{x}$ is obtained by conducting the IDFT modulation, a CP with length L is inserted, and the resulting complex base-band transmitted signal $\mathbf{s}$ can be expressed as

$$\mathbf{s} = \mathbf{G_I} \cdot \mathbf{x} = \mathbf{G_I} \cdot \mathbf{F_I} \cdot \mathbf{X} \in \mathbf{C}^{(N+L) \times 1}, \tag{39}$$

where

$$\mathbf{G_I} = \begin{bmatrix} \mathbf{0}_{L \times (N-L)} & & \mathbf{I}_L \\ & \mathbf{I}_N & \end{bmatrix} \in N^{(N+L) \times N},$$

$\mathbf{G_I}$ is the matrix for CP insertion, $\mathbf{I}$ is an identity matrix of the size noted in the subscript and $\mathbf{0}$ is a matrix of the size noted in the subscript whose entries are all zeros. The transmitted signal $\mathbf{s}$ is fed into a parallel-to-serial (P/S) operator, a digital-to-analog converter (DAC), a symbol shaping filter and finally an RF modulator for transmission. For complex base-band signals, the equivalent base-band representation of a multipath channel can be expressed as $\tilde{h}(\tau, t) = \sum_{m'} h_{m'}(t) \, \delta(\tau - \tau_{m'})$, where t denotes the time parameter, $h_{m'}(t)$ represents the m'th tap-weighting coefficient and τ is the delay parameter. The above 2-parameter channel model obeys the wide-sense stationary uncorrelated scattering (WSSUS) assumption. Based on the WSSUS and quasi-stationary assumptions, the channel tap-weighting coefficients are time-varying but do not change significantly within a single OFDM block duration of length NT_s, where T_s is the sampling period. Because the fractional durations (i.e., in a fraction of T_s) of delays are not taken into consideration, for a given time instant the above-mentioned tapped-delay-line channel model can be thought of as a CIR. Therefore, the channel model can be rewritten in a discrete-time representation for simplicity as $\mathbf{h} = \{h_m\} \in \mathbf{C}^{M \times 1}$, where M depends on the multipath delay spread. MT_s is thus the longest path delay; M varies according to the operating environment and cannot be known a priori at the receiving end. The received OFDM symbols can then be written in the following vector representation: $\mathbf{r}' = \mathbf{s} * \mathbf{h} + \mathbf{w}'$, where $*$ denotes the convolution operation, $\mathbf{r}' \in \mathbf{C}^{(N+L+M-1) \times 1}$ and $\mathbf{w}'$ is an AWGN vector whose elements are IID zero-mean Gaussian random variables with variance σ_w^2.

While in practice a residual timing error ϑ may occur with the employed symbol timing synchronization mechanism, the steady-state-response portion of $\mathbf{r}'$ can hopefully be obtained from

$$\mathbf{r}_\vartheta = \mathbf{G}_{\mathbf{R}, \vartheta} \cdot \mathbf{r}', \qquad \mathbf{G}_{\mathbf{R}, \vartheta} = \begin{bmatrix} \mathbf{0}_{N \times (L-\vartheta)} & \mathbf{I}_N & \mathbf{0}_{N \times (M+\vartheta-1)} \end{bmatrix}. \tag{40}$$

If the residual timing error ϑ in the above equation falls within $[0, L - M]$, there is no ISI in the received signal. In practice, ϑ may be only a few samples long and may be less than M, and $\vartheta = 0$ represents perfect synchronization. The demodulation process at the receiving end can be performed by means of a DFT operation, and the received signal vector should thus be transformed back into the sub-carrier space, i.e.,

$$\mathbf{R}_\vartheta = \mathbf{F_T} \cdot \mathbf{r}_\vartheta \in \mathbf{C}^{N \times 1}, \tag{41}$$

where

$$\mathbf{F_T} = \{f'_{k,n}\} \in \mathbf{C}^{N \times N},$$
$$f'_{k,n} = \frac{1}{\sqrt{N}} \exp\left(-j2\pi kn / N\right), \quad n = 0,1,\cdots,N-1; \quad k = 0,1,\cdots,N-1.$$

Moreover, $\mathbf{F_T}$ is the complex conjugate of $\mathbf{F_I}$ defined below Equation 37 and denotes the DFT matrix. Thus, the demodulated signals $\mathbf{R}_\vartheta$ on the sub-channels are obtained by the DFT operation, as shown in Equation 41. In addition, some specific components of $\mathbf{R}_\vartheta$ represent the outputs of the transmitted pilot symbols that pass through the corresponding pilot sub-channels. These entries of $\mathbf{R}_\vartheta$, i.e., R_k^ϑ, $k \in \zeta_p$, are exploited to estimate the pilot sub-channel by FDLS estimation, LMMSE or a complexity-reduced LMMSE via SVD, as shown in the previous section. After the pilot sub-channel gains have been estimated by FDLS, LMMSE or SVD, smoothing or interpolation/extrapolation methods are used to filter out the estimates of the data sub-channel gains from inter-path interference (IPI), ICI and noise. The previously mentioned pilot sub-channel estimation and data sub-channel interpolation/extrapolation can often be considered to be an up-sampling process conducted in the FD and can therefore be performed fully on the sub-channel space studied in Section 3.

As a matter of fact, the studied technique exploits a TD LS (TDLS) method to estimate the leading channel tap-weighting coefficients in the CIR, performs zero-padding to form an N-element vector and finally conducts the DFT operation on the resultant vector to effectively smooth in the FD. The studied technique accomplishes ideal interpolation with the domain transformation method used previously (Zhao & Huang, 1997). The whole CTF, including all of the channel gains on the pilot, data and virtual sub-channels over the entire occupied frequency band, can therefore be estimated simultaneously. The multipath delay spread of the transmission channel is typically dynamic and cannot be determined a priori at the receiving end. Therefore, the number of channel tap-weighting coefficients is often assumed to be less than L to account for the worst ISI-free case. The training sequence $\bar{\mathbf{x}}$ in the time direction, which is actually IDFT-transformed from the N_p in-band pilot symbols, has a period of approximately $\frac{N}{Q}$ because the pilot sub-channels are equally spaced by Q sub-channels. Therefore, the studied technique based on CTPA can effectively estimate at most the leading $\frac{N}{Q}$ channel tap-weighting coefficients. Meanwhile, in accordance with the Karhunen-Loève (KL) expansion theorem (Stark & Woods, 2001), the training sequence $\bar{\mathbf{x}}$ can be considered to be a random sequence with N_p degrees of freedom. Therefore, the order of the TDLS technique studied in this section can be conservatively determined to be at most N_p because $\bar{\mathbf{x}}$ can be exploited to sound a channel with an order less than or equal to N_p. Based on the above reasoning, the number of channel tap-weighting coefficients is assumed to be less than or equal to N_p, and the longest excess delay is thus assumed to be less than $N_p T_s$. Therefore, the received signals $\mathbf{r}_\vartheta$ can be reformulated as

$$\mathbf{r}_\vartheta = \mathbf{c}_\vartheta \cdot \mathbf{g} + \mathbf{w}_\vartheta = \overline{\mathbf{c}}_\vartheta \cdot \mathbf{g} + \tilde{\mathbf{w}}_\vartheta, \tag{42}$$

where $\mathbf{c}_\vartheta = \overline{\mathbf{c}}_\vartheta + \tilde{\mathbf{c}}_\vartheta$; $\tilde{\mathbf{w}}_\vartheta = \tilde{\mathbf{c}}_\vartheta \cdot \mathbf{g} + \mathbf{w}_\vartheta$;

$$\mathbf{c}_\vartheta = \left\{ c_{p,q}^\vartheta \right\} \in \mathbf{C}^{N \times N_p}, \qquad c_{p,q}^\vartheta = x_{|p-\vartheta-q|_N} = \overline{x}_{|p-\vartheta-q|_N} + \tilde{x}_{|p-\vartheta-q|_N},$$

$$\overline{\mathbf{c}}_\vartheta = \left\{ \overline{c}_{p,q}^\vartheta \right\} \in \mathbf{C}^{N \times N_p}, \qquad \overline{c}_{p,q}^\vartheta = \overline{x}_{|p-\vartheta-q|_N},$$

$$\tilde{\mathbf{c}}_\vartheta = \left\{ \tilde{c}_{p,q}^\vartheta \right\} \in \mathbf{C}^{N \times N_p}, \qquad \tilde{c}_{p,q}^\vartheta = \tilde{x}_{|p-\vartheta-q|_N},$$

$$0 \le p \le N-1, \qquad 0 \le q \le N_p - 1;$$

$\mathbf{c}_\vartheta$ is an $N \times N_p$ circulant matrix, and its left-most column is represented by

$$\mathrm{column}_0 \left(\mathbf{c}_\vartheta \right) = \begin{bmatrix} x_{|N-\vartheta|_N} & x_{|N+1-\vartheta|_N} & \cdots & x_{|N-1-\vartheta|_N} \end{bmatrix}^T;$$

$\mathbf{w}_\vartheta = \{w_{k-\vartheta}\} \in \mathbf{C}^{N \times 1}$ is an AWGN vector whose N elements, $w_{k-\vartheta}$, $k = L, L + 1, \cdots, L + N - 1$, are IID zero-mean Gaussian random variables with variance σ_w^2; and $\mathbf{g} = \{g_m\} \in \mathbf{C}^{N_p \times 1}$ contains the effective components that represent the channel tap-weighting coefficients. If no residual timing error exists, i.e., $\vartheta = 0$, then $g_m = h_m$, $m = 0,1, \cdots, M-1$ and $g_m = 0$, $M \le m < N_p$. Here $M \le N_p$, and at least $(N_p - M)$ components in $\mathbf{g}$ must be zeros due to the lack of precise information about M at the receiving end, especially given that mobile OFDM communication systems often operate on a rapidly time-varying channel. As a result, the CIR can be estimated by means of a standard over-determined LS method, i.e.,

$$\hat{\mathbf{g}}^{\mathrm{TDLS}} = \left\{ \hat{g}_m^{\mathrm{TDLS}} \right\} = \left(\overline{\mathbf{c}}_0^H \overline{\mathbf{c}}_0 \right)^{-1} \overline{\mathbf{c}}_0^H \cdot \mathbf{r}_\vartheta \in \mathbf{C}^{N_p \times 1}, \tag{43}$$

where the superscript $(\cdot)^H$ denotes a Hermitian operator, and

$$\overline{\mathbf{c}}_0 = \left\{ \overline{c}_{p,q}^0 \right\} \in \mathbf{C}^{N \times N_p}, \quad \overline{c}_{p,q}^0 = \overline{x}_{|p-q|_N}, \quad 0 \le p \le N-1, \qquad 0 \le q \le N_p - 1.$$

In practice, a residual timing error that occurs in the DFT demodulation process inherently leads to phase errors in rotating the demodulated symbols. The phase errors caused by a timing error ϑ are linearly dependent on both the timing error ϑ and the sub-channel index k. Any small residual timing error can severely degrade the transmission performance in all of the previous studies that exploit two-stage CTPA CEs (Hsieh & Wei, 1998; Edfors et al., 1998; Seller, 2004; Edfors et al., 1996; Van de Beek et al., 1995; Park et al., 2004; Zhao & Huang, 1997). On the other hand, the studied technique has a higher level of tolerance to timing errors. Because the timing error ϑ that occurs with the received training sequence (i.e., delayed replica of $\overline{\mathbf{x}}$) is the same as the error that occurs with the received data sequence (i.e., delayed replica of $\tilde{\mathbf{x}}$), the extra phase errors inserted into the demodulated symbols on individual sub-channels are the same as those that occur in the estimates of the sub-channel gains. Therefore, the extra phase rotations in the studied technique can be completely removed in the succeeding single-tap equalization process conducted on individual sub-channels. As a result, the studied technique can effectively deal with the problems caused by a residual timing error.

4.3 Remarks

The TD LS CE technique for OFDM communications has been studied in practical mobile environments. The studied TDLS technique based on the CTPA can accurately estimate the CIR and effectively track rapid CIR variations and can therefore achieve low error probabilities. A generic estimator is also performed sequentially on all OFDM blocks without assistance from a priori channel information and without increasing the computational complexity. Furthermore, the studied technique also exhibits better robustness to residual timing errors that occur in the DFT demodulation.

Whether OFDM communication should employ FD CE or TD CE has become an endless debate, because FD CE and equalization have attracted significant attention in recent years. While the LS method is not new, the TD CE may also not be considered novel. Although authors of some other publications thought that TDLS CE was not important, this must be a misunderstanding, and this section provides a very practical study. The material studied in this section has been deeply investigated in a previous study and its references (Lin, 2008c). This author strongly encourages interested readers, especially practical engineers and potential researchers, to examine the study and references closely to gain a deeper understanding of the applicability and practical value of the OFDM TD LS CE.

5. Channel estimation based on block pilot arrangement

5.1 Preliminary

The preceding two sections describe CE techniques based on the CTPA and taking advantage of either FD estimation or TD estimation methods. A CE technique based on the BTPA is discussed in this section. SC-FDMA has been chosen in the LTE specifications as a promising uplink transmission technique because of its low PAPR. Moreover, SC-FDM systems can be considered to be pre-coded OFDM communication systems, whose information symbols are pre-coded by the DFT before being fed into a conventional OFDMA (Myung et al., 2006).

In practice, pilot signals or reference signals for CE in SC-FDMA systems are inserted to occupy whole sub-channels periodically in the time direction, which can be considered to be BTPA. In this section, the signal model and system description of a BTPA-based CE technique is studied. The material discussed in this section can be found, in part, in a previous study (Huang & Lin, 2010).

5.2 System description

The information-bearing Gray-encoded symbols $\chi_u[n]$, $n = 0,1, \cdots, N_u - 1$ are pre-spread by an N_u-point DFT to generate the FD symbols $X_u[\kappa]$, $\kappa = 0,1, \cdots, N_u - 1$, i.e.,

$$X_u[\kappa] = \frac{1}{\sqrt{N_u}} \sum_{n=0}^{N_u-1} \chi_u[n] e^{-j2\pi n\kappa/N_u}, \quad \begin{array}{l} \kappa = 0,1,\cdots,N_u - 1, \\ u = 0,1,\cdots,U - 1, \end{array} \tag{44}$$

where U denotes the number of the users transmitting information toward the base-station, u denotes the user index, N_u denotes the sub-channel number which the uth user occupies, n denotes the time index and κ denotes the sub-carrier index. For a localized chunk arrangement used in the LTE specification, $X_u[\kappa]$, $\kappa = 0,1, \cdots, N_u - 1$ are allocated onto N_u sub-channels, i.e.,

$$S_u[k] = \begin{cases} X_u[\kappa], & k = \Gamma_u(\kappa) = \sum_{i=0}^{u-1} N_i + \kappa \\ 0, & k \neq \Gamma_u(\kappa), \quad \kappa = 0,1,\cdots,N_u-1. \end{cases} \tag{45}$$

The transmitted signal of the uth user is given by

$$s_u[n] = \frac{1}{\sqrt{N}} \sum_{k=0}^{N-1} S_u[k] e^{j2\pi kn/N}, \quad \begin{array}{l} n = 0,1,\cdots,N-1; \\ u = 0,1,\cdots,U-1. \end{array} \tag{46}$$

The signal received at the base-station can be expressed as

$$r[n] = \sum_{u=0}^{U-1} \sum_{m=0}^{M-1} h_u[m,n] s_u[n-m] + w[n], \quad n = 0,1,\cdots,N-1, \tag{47}$$

where $h_u[m,n]$ is the sample-spaced channel impulse response of the mth resolvable path on the time index n for the uth user, M denotes the total number of resolvable paths on the frequency-selective fading channel and $w[n]$ is AWGN with zero mean and a variance of σ_w^2. The time-varying multipath fading channel considered here meets the WSSUS assumption. Therefore, the channel-weighting coefficient $h_u[m,n]$ is modelled as a zero-mean complex Gaussian random variable, with an autocorrelation function that is written as

$$\mathrm{E}\left\{h_u[m,n]h_u^*[k,l]\right\} = \sigma_u^2[m] J_0\left(2\pi\nu_u|n-l|T_s\right)\delta[m-k], \tag{48}$$

where $\delta[\cdot]$ denotes the Dirac delta function, $J_0(\cdot)$ denotes the zeroth-order Bessel function of the first kind, ν_u denotes the maximum Doppler frequency of the uth user and $\sigma_u^2[m]$ denotes the power of the mth resolvable path on the channel that the uth user experiences. In addition, it is assumed in the above equation that the channel tap-weighting coefficients on different resolvable paths are uncorrelated and that the channel tap-weighting coefficients on an individual resolvable path have the Clarke's Doppler power spectral density derived by Jakes (Jakes & Cox, 1994). To simplify the formulation of Equation 47, it is assumed that timing synchronization is perfect, ISI can be avoided and CP can be removed. At the receiving end, the FFT demodulation is conducted, and the received TD signal $r[n]$ is thus transformed into the FD for demultiplexing, i.e.,

$$\begin{aligned} R[k] \quad &= \frac{1}{\sqrt{N}} \sum_{n=0}^{N-1} r[n] e^{-j2\pi nk/N} \\ &= \sum_{u=0}^{U-1} \bar{H}_{u,N/2}[k] S_u[k] + W[k], \qquad k = 0,1,\cdots,N-1, \end{aligned} \tag{49}$$

where

$$\bar{H}_{u,N/2}[k] \quad \doteq H_u[k,n], \qquad\qquad\qquad n = 0,1,\cdots,N-1,$$

$$H_u[k,n] \quad = \frac{1}{\sqrt{N}} \sum_{m=0}^{N-1} h_u[m,n] e^{-j2\pi mk/N}, \qquad \forall k = \Gamma_u(\kappa),$$

$$W[k] \quad = \frac{1}{\sqrt{N}} \sum_{n=0}^{N-1} w[n] e^{-j2\pi nk/N}, \qquad k = 0,1,\cdots,N-1.$$

In conventional FD CE, the weighting coefficient on the kth sub-channel $\bar{H}_{u,N/2}[k]$ is estimated by the FD LS CE, i.e.,

$$\hat{H}_{\text{FDLS}}[k] = \frac{R[k]S_p^*[k]}{\left|S_p[k]\right|^2}, \quad k = \Gamma_u(\kappa), \tag{50}$$

where $S_p[k]$ represents the pilot symbols in the FD, which are known a priori at the receiving end. In the LTE uplink, $S_p[k]$, $\forall k$ are obtained by transforming a Zadoff-Chu sequence onto the sub-carrier domain. Several CE techniques have been discussed in greater detail in a previous study (Huang & Lin, 2010). When the CE conducted by taking advantage of the pilot block is complete, several interpolation (or extrapolation) methods are conducted in the time direction to effectively smooth (or predict) the CTF or CIR upon transmission of the information-bearing symbols.

6. Channel estimation assisted from time-domain redundancy

6.1 Preliminary
To illustrate CE assisted by TD redundancy, a LS CE technique is studied in this section. The studied technique can apply pseudo-random-postfix orthogonal-frequency-division multiplexing (PRP-OFDM) communications to mobile applications, which often operate on a rapidly time-varying frequency-selective fading channel. Because conventional techniques that exploit a moving-average filter cannot function on a rapid time-varying channel, the studied technique takes advantage of several self-interference cancellation (SIC) methods to reduce IPI, ISI and IBI effectively and in a timely manner. The studied technique can thus overcome frequency selectivity caused by multipath fading and time selectivity caused by mobility; in particular, OFDM communication is often anticipated to operate in environments where both wide Doppler spreads and long delay spreads exist. Because conventional techniques based on MMSE CE usually require a priori channel information or significant training data, the studied method exploits a generic estimator assisted by LS CE that can be performed serially, block by block, to reduce computational complexity.

6.2 System description
The ith $N \times 1$ digital input vector $\mathbf{X}_N[i]$ is first modulated at the transmitting end with an IDFT operation. Thus, the TD information-bearing signal block can be expressed as

$$\mathbf{x}'_N[i] = \mathbf{F}_N^H \mathbf{X}_N[i], \tag{51}$$

where $\mathbf{X}_N[i]$ contains $2K \leq N$ QPSK-mapping information-bearing symbols;

$$\mathbf{F}_N = \frac{1}{\sqrt{N}}\left\{W_N^{kl}\right\}, \qquad W_N = e^{-j2\pi/N}, \qquad 0 \leq k < N, \quad 0 \leq l < N.$$

Immediately after the IDFT modulation process, a postfix vector $\mathbf{c}'_L = [c_0 \ c_1 \ \cdots \ c_{L-1}]^T$ is appended to the IDFT modulation output vector $\mathbf{x}'_N[i]$. In this section, $\mathbf{c}'_L$ is sifted from a partial period of a long pseudo-random sequence, and $\mathbf{c}'_L$ is phase-updated at every frame that contains several TD OFDM signal blocks, rather than using a deterministic postfix vector with a pseudo-random weight as in the conventional PRP-OFDM (Muck et al., 2006;

2005; 2003). This change is desirable when considering that previous works did not suggest long PRP sequences (Muck et al., 2006; 2005; 2003) and that pseudo-random sequences, e.g., the m-sequences or Gold sequences, are actually more general in various communication applications. Therefore, the ith transmitted block, with a length of $\Xi = N + L$, can be expressed as

$$\mathbf{x}_\Xi[i] = \mathbf{F}_{zp}^H \mathbf{X}_N[i] + \mathbf{c}_\Xi, \tag{52}$$

where

$$\mathbf{F}_{zp}^H = \begin{bmatrix} \mathbf{I}_N \\ \mathbf{0}_{L \times N} \end{bmatrix} \mathbf{F}_N^H, \quad \mathbf{c}_\Xi = \begin{bmatrix} \mathbf{0}_{N \times 1} \\ \mathbf{c}'_{L \times 1} \end{bmatrix}_{\Xi \times 1},$$

$\mathbf{I}_N$ denotes an $N \times N$ identity matrix and $\mathbf{0}_{L \times N}$ denotes a zero matrix of the size indicated in the subscript. The elements of $\mathbf{x}_\Xi[i]$ are then transmitted sequentially one by one (probably with transmit filtering or symbol shaping).

The channel studied here is modelled with a tapped-delay line of order $v - 1$, i.e., the impulse response of the investigated channel can be written as $\mathbf{h} = [h_0 \ h_1 \ \cdots \ h_{v-1}]^T$. It is commonly assumed that the length of the postfix (or prefix) L is larger than the length of the channel impulse response v. Typically, the multipath delay spread of the transmission channel is dynamic and cannot be determined a priori at the receiving end. Therefore, the number of channel tap-weighting coefficients is often assumed to be up to L to consider the worst ISI-free case, i.e., $v = L$. Thus, the longest excess delay is vT_s, where T_s denotes the sample duration.

At the receiving end, the ith OFDM symbol block can be formulated as

$$\mathbf{r}_\Xi[i] = \left(\mathbf{h}_{IBI,\Xi} + \mathbf{h}_{ISI,\Xi} \right) \mathbf{x}_\Xi[i] + \mathbf{w}_\Xi[i], \tag{53}$$

where $\mathbf{h}_{IBI,\Xi}$ is an $\Xi \times \Xi$ Toeplitz upper-triangular matrix in which the upper-most row is represented by

$$\text{row}_0 \left(\mathbf{h}_{IBI,\Xi} \right) = \begin{bmatrix} 0 \cdots 0 \, h_{v-1} \, h_{v-2} \cdots h_1 \end{bmatrix},$$

$\mathbf{h}_{ISI,\Xi}$ is an $\Xi \times \Xi$ Toeplitz lower-triangular matrix in which the left-most column is represented by

$$\text{column}_0 \left(\mathbf{h}_{ISI,\Xi} \right) = \begin{bmatrix} h_0 \, h_1 \cdots h_{v-1} \, 0 \cdots 0 \end{bmatrix}^T;$$

and $\mathbf{w}_\Xi[i]$ is the ith AWGN vector of elements with variance σ_w^2.

6.2.1 Channel estimation

In this section, the CIR is considered to be time-varying, but not significantly changing within one or two OFDM blocks. The symbols employed here in the CE can be written as follows:

$$\mathbf{r}_{CE,L+v-1}[i] = \begin{bmatrix} \langle \mathbf{r}_\Xi[i-1]_{N:\Xi-1} \rangle \\ \langle \mathbf{r}_\Xi[i] \, _{0:v-2} \rangle \end{bmatrix}_{(L+v-1) \times 1}, \tag{54}$$

where $\langle\mathbf{A}\rangle_{p:q}$ denotes either a column vector with elements arranged as $[A_p \ A_{p+1} \ \cdots \ A_q]^T$, sifted from a column vector $\mathbf{A}$, or a row vector with elements arranged as $[A_p \ A_{p+1} \ \cdots \ A_q]$, sifted from a row vector $\mathbf{A}$. In fact, $\mathbf{r}_{\text{CE},L+v-1}[i]$ can be reformulated in detail as follows:

$$\mathbf{r}_{\text{CE},L+v-1}[i] = \mathbf{C}[i]\mathbf{h} + \mathbf{w}''[i] = \mathbf{C}_\text{o}\mathbf{h} + \mathbf{w}'[i], \tag{55}$$

where $\mathbf{w}''[i]$ is an $(L + v - 1) \times 1$ AWGN vector of elements whose variances are σ_w^2;

$$\mathbf{C}[i] = \left(\mathbf{C}_\text{L}[i] + \mathbf{C}_\text{o} + \mathbf{C}_\text{U}[i]\right),$$

$\mathbf{C}_\text{o}$ is an $(L + v - 1) \times v$ Toeplitz matrix in which the left-most column is represented by

$$\text{column}_0\left(\mathbf{C}_\text{o}\right) = \begin{bmatrix} c_0 & c_1 & \cdots & c_{L-1} & 0 & \cdots & 0 \end{bmatrix}^T;$$

$\mathbf{C}_\text{U}[i]$ is an $(L + v - 1) \times v$ upper-triangular Toeplitz matrix in which the upper-most row is represented by

$$\text{row}_0\left(\mathbf{C}_\text{U}[i]\right) = [0 \ \langle\mathbf{x}_\Xi[i-1]\rangle_{N-1:N-(v-1)}];$$

$\mathbf{C}_\text{L}[i]$ is an $(L + v - 1) \times v$ lower-triangular Toeplitz matrix in which the left-most column is represented by

$$\text{column}_0\left(\mathbf{C}_\text{L}[i]\right) = [\mathbf{0}_{1 \times L} \ \langle\mathbf{x}_\Xi[i]\rangle_{0:v-2}^T]^T;$$

and

$$\mathbf{w}'[i] = \mathbf{w}''[i] + \mathbf{C}_\text{L}[i]\mathbf{h} + \mathbf{C}_\text{U}[i]\mathbf{h}.$$

In the above equation, $\mathbf{C}_\text{L}[i]\mathbf{h}$ results in ISI extending from on-time symbols onto the CE. Meanwhile, $\mathbf{C}_\text{U}[i]\mathbf{h}$ leads to IBI extending from preceding symbols onto the CE. In accordance with the LS philosophy (Stark & Woods, 2001; Kay, 1993), the CE studied here can thus be formulated as

$$\hat{\mathbf{h}}_\mathbf{0}[i] = \left(\mathbf{C}_\text{o}{}^H\mathbf{C}_\text{o}\right)^{-1}\mathbf{C}_\text{o}{}^H\overline{\mathbf{r}}_{\text{CE},L+v-1}[i], \tag{56}$$

where

$$\overline{\mathbf{r}}_{\text{CE},L+v-1}[i] = \frac{1}{2}\left(\mathbf{r}_{\text{CE},L+v-1}[i] + \mathbf{r}_{\text{CE},L+v-1}[i+1]\right).$$

In fact, the CE performed using $\overline{\mathbf{r}}_{\text{CE},L+v-1}[i]$ forces the channel estimator $\hat{\mathbf{h}}_\mathbf{0}[i]$, derived in Equation 56, to effectively exploit the first-order statistics to conduct the TD LI as employed in a previous work (Ma et al., 2006). Because of the LS philosophy, the statistics of $\mathbf{w}'[i]$ need not be completely known prior to performing the CE and $(\mathbf{C}_\text{o}{}^H\mathbf{C}_\text{o})^{-1} \ \mathbf{C}_\text{o}{}^H$ can be pre-calculated and pre-stored as a generic LS CE to reduce complexity. Furthermore, by taking advantage of decision-directed (DD) SIC, estimates of the CIR can be iteratively obtained by

$$\hat{\mathbf{h}}_\mathbf{1}[i] = \{(\mathbf{C}_\text{o}{}^H\mathbf{C}_\text{o})^{-1}\mathbf{C}_\text{o}{}^H\}\tilde{\mathbf{r}}_{\text{CE},L+v-1}[i], \tag{57}$$

where

$$\tilde{\mathbf{r}}_{\text{CE},L+v-1}[i] = \frac{1}{2}\left(\mathbf{r}_{\text{CE},L+v-1}[i] - \hat{\mathbf{C}}_{\text{U}}[i-1]\hat{\mathbf{h}}_1[i-1] + \mathbf{r}_{\text{CE},L+v-1}[i+1]\right), \quad i \geq 1;$$

$$\hat{\mathbf{h}}_1[0] = \hat{\mathbf{h}}_0[0]; \qquad \hat{\mathbf{C}}_{\text{U}}[0]\hat{\mathbf{h}}_1[0] = \mathbf{0}_{(L+v-1)\times 1} \text{ (initialization)};$$

and $\hat{\mathbf{C}}_{\text{U}}[i-1]$ denotes an $(L+v-1)\times L$ upper-triangular Toeplitz matrix in which the upper-most row is $[0 \ \langle\hat{\mathbf{x}}_\Xi[i-1]\rangle_{N-1:N-(v-1)}]$, which results from the DD symbols. Eventually, the estimates of sub-channel gains in individual frequency bins can be obtained by performing the DFT on the zero-padded replicas of either $\hat{\mathbf{h}}_0[i]$ or $\hat{\mathbf{h}}_1[i]$, i.e.,

$$\widehat{\mathbf{H}}_k[i] = \mathbf{F}_N \begin{bmatrix} \mathbf{I}_v & \mathbf{0}_{v\times(N-v)} \\ \mathbf{0}_{(N-v)\times v} & \mathbf{0}_{(N-v)\times(N-v)} \end{bmatrix} \hat{\mathbf{h}}_k[i], \quad k = 0,1. \tag{58}$$

6.2.2 Symbol recovery

For information detection at the receiving end, the ith information symbol within the DFT window can be obtained as

$$\mathbf{r}_{\text{SD},N}[i] = \langle\mathbf{r}_\Xi[i]\rangle_{0:N-1}, \tag{59}$$

and thus, its corresponding FD symbol is

$$\mathbf{R}_{\text{SD},0,N}[i] = \mathbf{F}_N\mathbf{r}_{\text{SD},N}[i]. \tag{60}$$

OLA: Based on the signal formatting in the PRP-OFDM communication under investigation, the ICI caused by various excess delays can be taken into account by modifying the signal symbol for signal detection to be

$$\mathbf{R}_{\text{SD},1,N}[i] = \mathbf{F}_N\left(\mathbf{r}_{\text{SD},N}[i] + \mathbf{r}_{\text{ICIc},N}[i]\right), \tag{61}$$

where

$$\mathbf{r}_{\text{ICIc},N}[i] = \begin{bmatrix} \langle\mathbf{r}_\Xi[i]\rangle_{N:N+v-2} \\ \mathbf{0}_{(N-v+1)\times 1} \end{bmatrix}$$

is exploited here for the purpose of ICI compensation. In fact, $\mathbf{R}_{\text{SD},1,N}[i]$ in Equation 61 can be considered to be a complexity-reduced variant modified from the method that was called the overlap-add (OLA) approach in previous studies (Muquest et al., 2002; Muck et al., 2003). It has been proven in previous studies (Muquet et al., 2000) that the OLA helps the ZP-OFDM achieve the same performance as the CP-OFDM because the OLA can reduce ICI by compensating for IPI and timing errors to maintain the orthogonality among sub-carriers, as in the CP-OFDM.

OLA with SIC: The conventional OLA mentioned above introduces some self-interference to the PRP-OFDM. Therefore, the self-interference occurring in the PRP-OFDM signal detection has to be eliminated. As a result, the signals fed into the detection can be formulated as

$$\mathbf{R}_{\mathrm{SD},2,\mathrm{k},N}[i] = \mathbf{F}_N \left(\mathbf{r}_{\mathrm{SD},N}[i] + \mathbf{r}_{\mathrm{ICIc},N}[i] - \hat{\mathbf{r}}_{\mathrm{prp},k}[i] \right), \quad k = 0,1,$$

where

$$\hat{\mathbf{r}}_{\mathrm{prp},k}[i] = \widetilde{\mathbf{C}}_{\mathrm{o}} \hat{\mathbf{h}}_k[i-1], \quad k = 0,1$$

and

$$\tilde{\mathbf{C}}_{\mathrm{o}} = \left\langle \tilde{\mathbf{C}}'_{\mathrm{o}} \right\rangle_{(v-1)\times v}$$

denotes a matrix containing the most upper-left $(v - 1) \times v$ elements of the matrix $\tilde{\mathbf{C}}'_{\mathrm{o}}$, which is a circulant matrix in which the left-most column is $[c_0 \, c_1 \, \cdots \, c_{L-1}]^T$.

6.3 Remarks

The LS CE technique has been thoroughly investigated in practical mobile environments. By taking advantage of SIC mechanisms, the studied technique can efficiently eliminate various interferences, accurately estimate the CIR, effectively track rapid CIR variations and, therefore, achieve low error probabilities. The studied technique can also achieve low bit error floors. The generic estimator assisted by LS CE can be performed sequentially on all OFDM blocks for complexity reduction without a priori channel information, which is required by conventional techniques based on MMSE. Several previous studies and their references regarding this topic are worth noting (Lin, 2009b;a; Lin & Lin, 2009; Lin, 2008b;a).

7. Summary

In this chapter, a variety of CE techniques on OFDM communications were investigated. This author does not attempt to present this topic in detail nor provide theoretical derivations and rigorous statistical analysis, though they are thought of as the most crucial for a journal publication. Insightful and reader-friendly descriptions are presented to attract readers of any level, including practicing communication engineers and beginning and professional researchers. All interested readers can easily find noteworthy materials in much greater detail from previous publications and the references cited in this chapter.

8. References

4MORE (2005). Eu-ist-4more project website, www.ist-4more.org .

Bingham, J. A. C. (1990). Multicarrier modulation for data transmission: an idea whose time has come, *IEEE Communications Magazine* Vol. 28(No. 5): 5–14.

Chang, R.W. (1966). Synthesis of band-limited orthogonal signals for multichannel data transmission, *Bell System Technical Journal* Vol. 45(No. 12): 1775–1796.

Chow, P. S. (1993). *Bandwidth Optimized Digital Transmission Techniques for Spectrally Shaped Channels with Impulse Noise*, Ph. D. Dissertation, Stanford University, CA.

Coleri, S., Ergen, M., Puri, A. & Bahai, A. (2002). Channel estimation techniques based on pilot arrangement in ofdm systems, *IEEE Transactions on Broadcasting* Vol. 48(No. 3): 223–229.

Couasnon, T. D., Monnier, R. & Rault, J. B. (1994). Ofdm for digital tv broadcasting, *Signal Processing* Vol. 39(No. 1-2): 1–32.

DAB (1995). Radio broadcasting systems; digital audio broadcasting (dab) to mobile, portable and fixed receivers, *European Telecommunications Standards* ETS 300 401, ETSI.

Darlington, S. (1970). On digital single-sideband modulators, *IEEE Transactions on Circuit Theory* Vol. 17(No. 3): 409–414.

DVB (1996). Digital broadcasting systems for television, sound and data services, *European Telecommunications Standards* prETS 300 744.

Edfors, O., Sandell, M., van de Beek, J.-J., Wilson, S. K. & Borjesson, P. O. (1996). Ofdm channel estimation by singular value decomposition, *Proceedings of IEEE 46th Vehicular Technology Conference, 1996*, IEEE Vehicular Technology Society, Atlanta, GA, pp. 923–927.

Edfors, O., Sandell, M., van de Beek, J.-J., Wilson, S. K. & Borjesson, P. O. (1998). Ofdm channel estimation by singular value decomposition, *IEEE Transactions on Communications* Vol. 46(No. 7): 931–939.

Elliott, D. F. (1988). *Handbook of Digital Signal Processing: Engineering Applications,* Academic Press.

Fazel, K. (1994). Performance of convolutionally coded cdma/ofdm in a frequency-time selective fading channel and its near-far resistance, *Proceedings of IEEE International Conference on Communications, 1994. ICC'94*, IEEE Communications Society, New Orleans, LA, pp. 1438 – 1442.

Floch, B. L., Alard, M. & Berrou, C. (1995). Coded orthogonal frequency division multiplex [tv broadcasting], *Proceedings of the IEEE* Vol. 86(No. 6): 982–996.

Gui, L., Li, Q., Liu, B., Zhang, W. & Zheng, C. (2009). Low complexity channel estimation method for tds-ofdm based chinese dttb system, *IEEE Transactions Consumer Electronics* Vol. 55(No. 3): 1135–1140.

Han, K.-Y., Lee, S.-W., Lim, J.-S. & Sung, K.-M. (2004). Channel estimation for ofdm with fast fading channels by modified kalman filter, *IEEE Transactions on Consumer Electronics* Vol. 50(No. 2): 443–449.

Hara, S. & Prasad, R. (1997). Multicarrier modulation for data transmission: an idea whose time has come, *IEEE Communications Magazine* Vol. 35(No. 12): 126–133.

Hoeher, P. (1991). Tcm on frequency-selective land-mobile fading channels, *Proceedings of International Workshop Digital Communications*, Tirrenia, Italy, pp. 317–328.

Hoeher, P., Kaiser, S. & Robertson, P. (1997). Two-dimensional pilot-symbol-aided channel estimation by wiener filtering, *Proceedings of 1997 IEEE International Conference on Acoustics, Speech, and Signal Processing (ICASSP'97)*, IEEE Signal Processing Society, Munich, pp. 1845–1848.

Hsieh, M.-H. & Wei, C.-H. (1998). Channel estimation for ofdm systems based on comb-type pilot arrangement in frequency selective fading channels, *IEEE Transactions on Consumer Electronics* Vol. 44(No. 1): 217–225.

Huang, S.-C. & Lin, J.-C. (2010). Novel channel estimation techniques on sc-fdma uplink transmission, *Proceedings of 2010 IEEE Vehicular Technology Conference (VTC 2010-Spring)*, IEEE Vehicular Technology Society, Taipei, Taiwan.

Jakes, W. C. & Cox, D. C. (1994). *Microwave Mobile Communications*, Wiley-IEEE Press.

Kay, S. M. (1993). *Fundamentals of Statistical Signal Processing, Volume I: Estimation Theory,* Prentice Hall; 1 edition.

Klerer, M. (2005). Ieee 802.20 websites, grouper.ieee.org/groups/802/20/.

Kondo, S. & Milstein, B. (1996). Performance of multicarrier ds cdma systems, *IEEE Transactions on Communications* Vol. 44(No. 2): 238–246.

Levanon, N. & Mozeson, E. (2004). *Radar Signals*, Wiley-IEEE Press.

Li, B., Xu, Y. & Choi, J. (2002). A study of channel estimation in ofdm systems, *Proceedings of 2002 IEEE 56th Vehicular Technology Conference, 2002 (VTC 2002-Fall)*, IEEE Vehicular Technology Society, Vancouver, Canada, pp. 894–898.

Li, B., Xu, Y. & Choi, J. (2008). Channel estimation for lte uplink in high doppler spread, *Proceedings of Wireless Communications and Networking Conference, 2008 (WCNC 2008)*, IEEE Communications Society, Las Vegas, NV, pp. 1126–1130.

Lin, J.-C. (2008a). Channel estimation assisted by postfixed pseudo-noise sequences padded with null samples for mobile ofdm communications, *Proceedings of IEEE Wireless Communications and Networking Conference, 2008 (WCNC 2008)*, IEEE Communications Society, Las Vegas, NV, pp. 846–851.

Lin, J.-C. (2008b). Least-squares channel estimation assisted by self-interference cancellation for mobile prp-ofdm applications, *Proceedings of IEEE International Conference on Communications, 2008 (ICC '08)*, IEEE Communications Society, Beijing, China, pp. 578– 583.

Lin, J.-C. (2008c). Least-squares channel estimation for mobile ofdm communication on time-varying frequency-selective fading channels, *IEEE Transactions on Vehicular Technology* Vol. 57(No. 6): 3538–3550.

Lin, J.-C. (2009a). Channel estimation assisted by postfixed pseudo-noise sequences padded with zero samples for mobile orthogonal-frequency-division-multiplexing communications, *IET Communications* Vol. 3(No. 4): 561–570.

Lin, J.-C. (2009b). Least-squares channel estimation assisted by self-interference cancellation for mobile prp-ofdm applications, *IET Communications* Vol. 3(No. 12): 1907–1918.

Lin, J.-C. & Lin, C.-S. (2009). Ls channel estimation assisted from chirp sequences in ofdm communications, *Proceedings of 1st International Conference on Wireless Communication, Vehicular Technology, Information Theory and Aerospace & Electronic Systems Technology, 2009 (Wireless VITAE 2009)*, IEEE ComSoc, ITS and VTS, Aalborg, Denmark, pp. 222–226.

Liu, G.-S. & Wei, C.-H. (1992). A new variable fractional sample delay filter with nonlinear interpolation, *IEEE Transactions on Circuits and Systems II: Analog and Digital Signal Processing* Vol. 39(No. 2): 123–126.

Liu, G. & Zhang, J. (2007). Itd-dfe based channel estimation and equalization in tds-ofdm receivers, *IEEE Transactions Consumer Electronics* Vol. 53(No. 2): 304–309.

LTE (2009). TS 36.211 (V8.5.0), *Physical Channels and Modulation*, 3GPP.

Ma, Y., Yi, N. & Tafazolli, R. (2006). Channel estimation for prp-ofdm in slowly time-varying channel: first-order or second-order statistics?, *IEEE Signal Processing Letters* Vol. 13(No. 3): 129–132.

Marks, R. B. (2008). Ieee 802.16 standard, www.ieee802.org/16/.

Marti, B., Bernard, P., Lodge, N. & Schafer, R. (1993). European activities on digital television broadcasting – from company to cooperative projects, *EBU Technical Review* Vol. 256: 20–29. www.ebu.ch/en/technical/trev/trev_256-marti.pdf.

MATRICE (2005). Eu-ist-matrice project website, www.ist-matrice.org .

Minn, H. & Bhargava, V. K. (1999). Channel estimation for ofdm systems with transmitter diversity immobile wireless channels, *IEEE Journal on Selected Areas in Communications* Vol. 17(No. 3): 461–471.

Minn, H. & Bhargava, V. K. (2000). An investigation into time-domain approach for ofdm channel estimation, *IEEE Transactions on Broadcasting* Vol. 46(No. 4): 240–248.

Moeneclaey, M. & Bladel, M. V. (1993). Digital hdtv broadcasting over the catv distribution system, *Signal processing: Image communication* Vol. 5(No. 5-6): 405–415.

Muck, M., de Courville, M., Debbah, M. & Duhamel, P. (2003). A pseudo random postfix ofdm modulator and inherent channel estimation techniques, *Proceedings of IEEE 2003 Global Telecommunications Conference (GLOBECOM '03)*, IEEE Communications Society, San Francisco, pp. 2380–2384.

Muck,M., de Courville, M. & Duhamel, P. (2006). A pseudorandom postfix ofdm modulator – semi-blind channel estimation and equalization, *IEEE Transactions on Signal Processing* Vol. 54(No. 3): 1005–1017.

Muck, M., de Courville, M., Miet, X. & Duhamel, P. (2005). Iterative interference suppression for pseudo random postfix ofdm based channel estimation, *Proceedings of 2005 IEEE International Conference on Acoustics, Speech, and Signal Processing (ICASSP'05)*, IEEE Signal Processing Society, Philadelphia, Pennsylvania, USA, pp. 765–768.

Muquest, B., Wang, Z., Giannakis, G. B., Courville, M. & Duhamel, P. (2002). Cyclic prefixing or zero padding for wireless multicarrier transmissions?, *IEEE Transactions on Communications* Vol. 50(No. 12): 2136–2148.

Muquet, B., de Courville, M., Giannakis, G. B., Wang, Z. & Duhamel, P. (2000). Reduced-complexity equalizers for zero-padded ofdm transmissions, *Proceedings of 2000 IEEE International Conference on Acoustics, Speech, and Signal Processing (ICASSP'00)*, IEEE Signal Processing Society, Istanbul, pp. 2973–2976.

Myung, H. G., Lim, J. & Goodman, D. J. (2006). Single carrier fdma for uplink wireless transmission, *IEEE Vehicular Technology Magazine* Vol. 1(No. 3): 30–38.

Negi, R. & Cioffi, J. (1998). Pilot tone selection for channel estimation in a mobile ofdm system, *IEEE Transactions on Consumer Electronics* Vol. 44(No. 3): 1122–1128.

Ng, J. C. L., Letaief, K. B. & Murch, R. D. (1998). Complex optimal sequences with constant magnitude for fast channel estimation initialization, *IEEE Transactions on Communications* Vol. 46(No. 3): 305–308.

Ohno, S. & Giannakis, G. B. (2002). Optimal training and redundant precoding for block transmissions with application to wireless ofdm, *IEEE Transactions on Communications* Vol. 50(No. 12): 2113–2123.

Park, J., Kim, J., Kang, C. & Hong, D. (2004). Channel estimation performance analysis for comb-type pilot-aided ofdm systems with residual timing offset, *Proceedings of IEEE 60th Vehicular Technology Conference, 2004 (VTC2004-Fall)*, IEEE Vehicular Technology Society, Los Angeles, CA, pp. 4376–4379.

Peled, A. & Ruiz, A. (1980). Frequency domain data transmission using reduced computational complexity algorithms, *Proceedings IEEE International Conference on Acoustics, Speech, and Signal Processing (ICASSP'80)*, IEEE Signal Processing Society, Denver, CO, pp. 964–967.

Popovic, B. M. (1992). Generalized chirp-like polyphase sequences with optimum correlation properties, *IEEE Transactions on Information Theory* Vol. 38(No. 4): 1406–1409.

Reiners, C. & Rohling, H. (1994). Multicarrier transmission technique in cellular mobile communication systems, *Proceedings of 1994 IEEE 44th Vehicular Technology Conference*, IEEE Vehicular Technology Society, Stockholm, pp. 1645–1649.

Rinne, J. & Renfors, M. (1996). Optimal training and redundant precoding for block transmissions with application to wireless ofdm, *IEEE Transactions Consumer Electronics* Vol. 42(No. 4): 959–962.

Saltzberg, B. (1967). Performance of an efficient parallel data transmission system, *IEEE Transactions on Communication Technology* Vol. 15(No. 6): 805–811.

Sandell, M. & Edfors, O. (1996). A comparative study of pilot-based channel estimators for wireless ofdm, *Research Report / 1996:19. Div. Signal Processing, Lulea Univ. Technology, Lulea, Sweden* Vol.(No.).

Seller, O. (2004). Low complexity 2d projection-based channel estimators for mc-cdma, *Proceedings of 15th IEEE International Symposium on Personal, Indoor and Mobile Radio Communications, 2004 (PIMRC 2004)*, IEEE Communications Society, Barselona, pp. 2283 – 2288.

Simeone, O., Bar-Ness, Y. & Spagnolini, U. (2004). Pilot-based channel estimation for ofdm systems by tracking the delay-subspace, *IEEE Transactions on Wireless Communications* Vol. 3(No. 1): 315–325.

Song, B., Gui, L., Guan, Y. & Zhang, W. (2005). On channel estimation and equalization in tds-ofdm based terrestrial hdtv broadcasting system, *IEEE Transactions Consumer Electronics* Vol. 51(No. 3): 790–797.

Sourour, E. A. & Nakagawa, M. (1996). Performance of orthogonal multicarrier cdma in a multipath fading channel, *IEEE Transactions on Communications* Vol. 44(No. 3): 356 – 367.

Stark, H. & Woods, J. W. (2001). *Probability and Random Processes with Applications to Signal Processing,* Prentice Hall, 3rd ed.

Steele, R. (1999). *Mobile Radio Communications*, John Wiley & Sons, Inc.

Tourtier, P. J., Monnier, R. & Lopez, P. (1993). Multicarrier model for digital hdtv terrestrial broadcasting, *Signal processing: Image communication* Vol. 5(No. 5-6): 379–403.

Tu, J. C. (1991). *Theory, Design and Application of Multi-Channel Modulation for Digital Communications,* Ph. D. Dissertation, Stanford University, CA.

Tufvesson, F. & Maseng, T. (1997). Pilot assisted channel estimation for ofdm in mobile cellular systems, *Proceedings of 1997 IEEE 47th Vehicular Technology Conference*, IEEE Vehicular Technology Society, Phoenix, AZ, pp. 1639–1643.

Van de Beek, J.-J., Edfors, O., Sandell, M., Wilson, S. K. & Borjesson, P. O. (1995). On channel estimation in ofdm systems, *Proceedings of 1995 IEEE 45th Vehicular Technology Conference*, IEEE Vehicular Technology Society, Chicago, IL, pp. 815–819.

Weinstein, S. B. & Ebert, P. M. (1971). Data transmission by frequency-division multiplexing using the discrete fourier transform, *IEEE Transactions on Communication Technology* Vol. 19(No. 5): 628–634.

Wilson, S. K., Khayata, R. E. & Cioffi, J. M. (1994). 16-qam modulation with orthogonal frequency-division multiplexing in a rayleigh-fading environment, *Proceedings of*

1994 IEEE 44th Vehicular Technology Conference, IEEE Vehicular Technology Society, Stockholm, pp. 1660–1664.

Yang, F., Wang, J., Wang, J., Song, J. & Yang, Z. (2008). Novel channel estimation method based on pn sequence reconstruction for chinese dttb system, *IEEE Transactions Consumer Electronics* Vol. 54(No. 4): 1583–1589.

Yeh, C.-S. & Lin, Y. (1999). Channel estimation techniques based on pilot arrangement in ofdm systems, *IEEE Transactions on Broadcasting* Vol. 45(No. 4): 400–409.

Young, G., Foster, K. T. & Cook, J. W. (1996). Broadband multimedia delivery over copper, *Electronics & Communication Engineering Journal* Vol. 8(No. 1): 25.

Zhao, Y. & Huang, A. (1997). A novel channel estimation method for ofdm mobile communication systems based on pilot signals and transform-domain processing, *Proceedings of 1997 IEEE 47th Vehicular Technology Conference*, IEEE Vehicular Technology Society, Phoenix, AZ, pp. 2089–2093.

Zheng, Z.-W. & Sun, Z.-G. (2008). Robust channel estimation scheme for the tds-ofdm based digital television terrestrial broadcasting system, *IEEE Transactions Consumer Electronics* Vol. 54(No. 4): 1576–1582.

Zou,W. Y. &Wu, Y. (1995). Cofdm: an overview, *IEEE Transactions on Broadcasting* Vol. 41(No. 1): 1–8.

Communications and Networking

Edited by Jun Peng

ISBN 978-953-307-114-5

Hard cover, 434 pages

Publisher Sciyo

Published online 28, September, 2010

Published in print edition September, 2010

This book "Communications and Networking" focuses on the issues at the lowest two layers of communications and networking and provides recent research results on some of these issues. In particular, it first introduces recent research results on many important issues at the physical layer and data link layer of communications and networking and then briefly shows some results on some other important topics such as security and the application of wireless networks. In summary, this book covers a wide range of interesting topics of communications and networking. The introductions, data, and references in this book will help the readers know more abut this topic and help them explore this exciting and fast-evolving field.

How to reference

In order to correctly reference this scholarly work, feel free to copy and paste the following:

Jia-Chin Lin (2010). Channel Estimation for Wireless OFDM Communications, Communications and Networking, Jun Peng (Ed.), ISBN: 978-953-307-114-5, InTech, Available from: http://www.intechopen.com/books/communications-and-networking/channel-estimation-for-wireless-ofdm-communications

INTECH
open science | open minds